

NASA TECHNICAL NOTE



NASA TN D-6517

C.1

LOAN COPY: RETURN TO
AFWL (DOUL)
KIRTLAND AFB, N. M.



NASA TN D-6517

MEASUREMENTS AND ANALYSIS OF
SOLID-PROPELLANT-ROCKET VIBRATIONS
OBTAINED DURING A CAPTIVE FLIGHT

by James A. Schoenster

Langley Research Center
Hampton, Va. 23365

NATIONAL AERONAUTICS AND SPACE ADMINISTRATION • WASHINGTON, D. C. • OCTOBER 1971



0133418

| | | | |
|-------------------------------------------------------------------------------------------------------------------------------------------------------------------------------------------------------------------------------------------------------------------------------------------------------------------------------------------------------------------------------------------------------------------------------------------------------------------------------------------------------------------------------------------------------------------------------------------------------------------------------------|--------------------------------------------------------|---------------------------------------------------------|----------------------|
| 1. Report No. NASA TN D-6517 | 2. Government Accession No. | 3. Recipient's Catalog No. | |
| 4. Title and Subtitle MEASUREMENTS AND ANALYSIS OF SOLID-PROPELLANT-ROCKET VIBRATIONS OBTAINED DURING A CAPTIVE FLIGHT | 5. Report Date October 1971 | 6. Performing Organization Code | |
| 7. Author(s) James A. Schoenster | 8. Performing Organization Report No. L-7837 | 10. Work Unit No. 114-08-13-03 | |
| 9. Performing Organization Name and Address NASA Langley Research Center Hampton, Va. 23365 | 11. Contract or Grant No. | 13. Type of Report and Period Covered Technical Note | |
| 12. Sponsoring Agency Name and Address National Aeronautics and Space Administration Washington, D.C. 20546 | 14. Sponsoring Agency Code | | |
| 15. Supplementary Notes | | | |
| 16. Abstract As part of an overall program to investigate the vibrational environment of small solid-propellant rockets, a captive test firing of a Nike rocket with a boilerplate payload was conducted in a unique test stand which, while restraining the total vehicle displacement, allowed substantial freedom for the test vehicle to vibrate. Measurements were obtained of the vibratory accelerations, pressures in the rocket case, rocket-case strains, and total vehicle displacement and data are presented. A discussion of the analytical procedures used to interpret random phenomena is presented. | | | |
| 17. Key Words (Suggested by Author(s)) Solid-propellant-rocket vibrations Random vibration analysis | 18. Distribution Statement Unclassified - Unlimited | | |
| 19. Security Classif. (of this report) Unclassified | 20. Security Classif. (of this page) Unclassified | 21. No. of Pages 39 | 22. Price* \$3.00 |

MEASUREMENTS AND ANALYSIS OF SOLID-PROPELLANT-ROCKET
VIBRATIONS OBTAINED DURING A CAPTIVE FLIGHT

By James A. Schoenster
Langley Research Center

SUMMARY

As part of an overall program to investigate the vibrational environment of small solid-propellant rockets, a captive test firing of a Nike rocket was conducted in a unique test stand. The stand was designed to allow the rocket to vibrate freely while the overall displacement of the vehicle due to static thrust was restrained. Measurements were made to determine the vibrational behavior of the vehicle, which included a boilerplate payload, and the effects of the test stand on the vehicle. These measurements included vibratory accelerations along the length of the vehicle, pressures in the rocket case, rocket-case strains, and total vehicle displacement. Data could be obtained only during a limited time period because of the short burn time of the rocket and, therefore, a discussion of the analytical procedures used by the working engineer to interpret these random phenomena is presented.

The test results demonstrated the ability of the test stand to meet all dynamic requirements; however, problems were encountered in measuring the oscillatory pressures generated during burning of the rocket due to the low level of these oscillations. The power-spectral-density vibration levels measured to 2000 Hz were considerably lower than those usually specified as flight environmental levels for solid-propellant rockets. High responses were experienced at frequencies above 10 000 Hz.

INTRODUCTION

A major problem in insuring the success of a space mission is to determine the dynamic loads which may affect the payload—launch-vehicle system and then to specify tests which will demonstrate the ability of the system to perform satisfactorily under those loads. Undertesting may not show potential defects which could compromise the success of the mission, whereas overtesting could lead to structural overdesign. The problems associated with overdesign, which may cost both time and money, are several; among these are weight restrictions on the payload which limit the objectives of the mission, the need for a larger launch vehicle to perform the mission, and additional design

effort to eliminate dynamic-response problems associated with individual components for each payload.

In spite of the problems of overdesign, vibration environment specifications on solid-propellant rockets usually are very conservative as a result of the lack of flight measurements (ref. 1). F. R. Wagner, in his studies on solid-propellant-rocket load definition, discussed the vibrational environment and concluded that the problems associated with overdesign are frequently encountered (in 1969 at the Solid Rocket Structural Integrity Information Center, University of Utah). Therefore, because of the uncertainties involved in defining test specifications, a strong need exists for adequate analytical and experimental methods for predicting flight vibration frequencies, amplitudes, and damping values.

In a Langley Research Center program measurements are being obtained of the flight vibrations on both a payload and its solid-propellant launch vehicle to aid in developing techniques for predicting vibrational environment. These flight measurements will be used for evaluating data obtained from a captive firing of the same payload—launch-vehicle combination in a special test stand to determine whether vibration measurements from a captive firing can be used to establish test specifications for flight hardware. A preliminary step in the program prior to either the captive firing or flight of the actual payload—launch-vehicle system was the firing of a combination of the boilerplate payload and the launch vehicle in the test stand with the following three objectives:

1. Obtain vibration data from the launch-vehicle—boilerplate—payload combination
2. Verify the capability of the instrumentation to obtain the necessary data
3. Verify the ability of the restraint system to allow the vehicle to vibrate freely while withstanding the rocket firing loads

It is the purpose of this report to present some results from this preliminary ground firing. The primary measurements obtained during this firing were restraining force on the rocket, vibratory accelerations at various locations on the vehicle, pressures in the solid-propellant rocket case, and acoustic levels in the test cell. Because much of the vibration data obtained was random in nature, the data evaluation methods are discussed in detail.

SYMBOLS

B bandwidth, Hz

dB decibel, root-mean-square pressure referenced to 2×10^{-5} N/m²

f frequency, Hz

| | |
|-------------|-----------------------------------------------------------------------------------|
| $f(t)$ | function of time |
| g | acceleration of gravity, 9.807 m/sec ² |
| k | statistical degrees of freedom |
| m | maximum number of time-lag values |
| n | sample size |
| $p(x)$ | probability-density function |
| $R_x(\tau)$ | autocorrelation function |
| T | record length, seconds |
| T_x | amount of time $x(t)$ falls inside the range from x to $x + \Delta x$, seconds |
| t | time, seconds |
| $x, x(t)$ | amplitude, g units, N/m ² , dB, μ m/m, cm, or N |
| Δf | change in frequency |
| Δt | change in time |
| Δx | change in amplitude |
| ϵ | sampling interval, seconds |
| μ_x | mean value, g units or N/m ² |
| σ_x | root-mean-square value, g units or N/m ² |
| τ | time-lag value, seconds |
| $\Phi_x(f)$ | power spectral density |
| χ^2 | chi-square probability distribution function |

Subscripts:

av average

meas measured

pk peak

rms root mean square

APPARATUS AND TEST CONDITIONS

Description of Test Vehicle

The vehicle used in this firing consisted of a Nike type M88, solid-propellant rocket and a boilerplate payload. The nominal rocket thrust was 213 000 N with a burning time of 3.4 sec. In order to be representative of the flight condition, the boilerplate payload was designed to bring the total weight of the vehicle to 705.2 kg with a center of gravity 2.05 m from the aft end of the Nike nozzle. The boilerplate payload was a steel cylinder 1.36 m long, 0.381 m in diameter, with a 0.3175-cm-thick wall. It had a 3.175-cm-thick plate at the forward end and six 2.54- by 0.635-cm longitudinal stiffeners equally spaced around its circumference. The boilerplate payload weighed approximately 83.4 kg. Shown in figure 1 is the test vehicle mounted in the test stand. Figures 2 to 6 show various details of the test vehicle.

Description of Test Stand

The test stand, shown in figure 1, is a built-up box-beam structure designed to support a launch vehicle with cables to three torsion bars as shown schematically in figure 2. The launch vehicle is shown in the nozzle-up position used for firing in this test stand. Three short cables, which are attached at the aft end of the Nike rocket case and which run over pulleys, connected the vehicle to the torsion bars. The torsion bars are spaced at 120° intervals around the thrust axis and have a combined stiffness of 10.33 kN/cm. The suspension-system natural frequency was experimentally verified by attaching a 705.2-kg load to the torsion bars. The resulting 6.1-Hz frequency agreed with a calculated value based on the assumption of a single-degree-of-freedom system. The damping of the suspension system under this load was experimentally determined to be 4 percent of an equivalent critically damped viscous system.

In addition to providing a restraining force which reacts to the thrust of the rocket, the test stand provides a preload which may be used to restrict the initial displacement of the rocket, as shown schematically in figure 2. Lateral restraint of the torsion bar is

provided by three bearings, two at the top and one at the bottom. A quarter sector at the top of the torsion bar is connected by a short cable over a pulley to a fitting at the aft end of the rocket. A rod, connected to the same fitting as the cable, passes through a hole in a test-stand brace beam and a block of honeycomb. A washer and two jam nuts on this rod hold the block of honeycomb against the brace beam. A preload turnbuckle at the base of the torsion bar, when adjusted, twists the torsion bar and thereby causes the rod to pull the honeycomb against the brace beam. The force in the cables caused by the torsion bars is measured by a force link located at the cable attachment to the rocket. When the rocket is fired, the vehicle does not unload the honeycomb until the preload condition is exceeded, at which time the rod is free to slide through the hole in the brace beam and release the load on the honeycomb. A spring-loaded spacer, shown in figure 2, is originally inserted between the honeycomb and the brace beam. After ignition, and after the honeycomb has been unloaded, the spacer is extracted by the springs, which allows the vehicle to oscillate past the initial rest point during the vibration set up by the initial impact of the rocket firing. This permits the use of higher preloads which further limit the initial acceleration and total displacement of the vehicle. At the end of the thrusting period, the vehicle moves upward under the influence of the torsion-bar force and the energy in the system is absorbed by the honeycomb. A photograph of the honeycomb-spacer installation is shown in figure 3.

Description of Instrumentation

Six types of instruments used during the ground firing test are the force link, displacement potentiometer, pressure transducer, crystal vibrometer, strain gage, and microphone. Listed in table I are the linear frequency range, the linear amplitude range, and the calibrate factors for each of the instruments. All data obtained from these instruments were recorded on magnetic tape. A brief description of the installation and location of these transducers is presented in the following paragraphs.

Force links.- Force links were placed between the cable and Nike attach fitting (fig. 4) to measure the preload and overall force on the torsion bars. Each link consists of a strain-gaged square steel rod, 2.032 cm across the flats and approximately 3.30 cm long.

Potentiometer.- In order to measure the mean position of the vehicle during firing, a linear-displacement potentiometer was attached between the test stand and a bracket bonded to the Nike case approximately 1.90 m from the forward thrust face of the Nike. (See fig. 5.)

Pressure transducers.- Three pressure transducers were installed in the Nike rocket case. Transducers 2 and 3 were flush mounted in the forward thrust dome of the Nike approximately 180° apart. Transducer 1 (fig. 4) was mounted in the convergent section of the nozzle. The signal from each transducer was divided into two parts. The part

of the signal referred to as the dc pressure measurement represents the total pressure at the transducer location. The part of the signal referred to as the ac pressure measurement is the same signal passed through a high-pass filter to remove the dc component and amplified $2\frac{1}{2}$ times. The recovery time of the amplifier for this part of the signal due to the initial pressure-pulse overload is 0.075 sec. In this paper, the two signals obtained from a single transducer are considered to be coming from independent transducers and are referred to as the dc pressure measurement and the ac pressure measurement.

Vibrometers.- Six vibrometers (vibration transducers) were mounted on the vehicle. Vibrometers 1 and 2 were mounted at the aft end of the Nike case (fig. 4) to measure longitudinal and tangential motions, respectively. Vibrometers 3 and 4 were mounted at the forward end of the Nike (fig. 6) for longitudinal and radial measurements, respectively. Vibrometer 5 was also mounted longitudinally at the forward end of the Nike case on an attachment bolt approximately 180° around the circumference from vibrometer 3. Vibrometer 6 was on the forward end of the boilerplate payload (fig. 7) to detect longitudinal response.

The vibrometers were crystal accelerometers using charge amplifiers and were mounted on thermal-electrical isolation studs. This vibration measuring system was checked on a calibration shaker to 10 000 Hz and the amplitude response was down 1.2 dB at that frequency.

Strain gages.- Three strain-gage bridge circuits were placed on the Nike to measure longitudinal strains. They were located 1 rocket-case diameter (0.406 m) away from the forward thrust face and spaced at 120° intervals.

Microphones.- Two microphones were mounted external to the vehicle. Microphone 1 was mounted near the nozzle end of the vehicle. (See fig. 4.) Microphone 2 was set near the midpoint of the boilerplate payload. (See fig. 6.)

DATA ANALYSIS TECHNIQUES

In general, the vibrations of the payload and solid-propellant launch vehicle are random in nature and require statistical methods for evaluating the response. Procedures for analyzing random signals from constant-parameter linear systems are available (for example, ref. 2) and have been used in studying of response in structures (ref. 3). Four main parameters are usually used to describe the basic properties of random data: (1) mean-square value, (2) power spectral density, (3) probability density, and (4) auto-correlation. A problem in using these parameters to evaluate the data from a rocket firing is that conventional techniques available are based on the assumption of a constant-parameter linear system with stationary inputs. Because the vehicle consumes an amount of fuel equal to approximately half its initial mass, there are definitely some time-varying

parameters. In addition, it is not known whether the input itself is a stationary process. Therefore, in order to use well-defined random-analysis techniques for stationary data, the concept of "self-stationarity" is applied. Self-stationarity assumes that the variation in the properties of the system will be less than the anticipated statistical variations due to the sampling theory.

The entire firing time for this rocket is nominally 3.4 sec; however, information of interest is not available during the initial shock transient, which lasts about 0.1 sec, due to instrumentation limitations. Also, in the test stand a preload will cause the vehicle to return to the stops on the stand before burnout of the rocket. Therefore, the data period in which the response of the vehicle is due only to the burning of the propellant with minimum restraints on the structure is from approximately 0.1 to 3 sec of the actual burn time. Analysis of the data was performed during this time period.

Information Obtained

Time history.- The data are presented on oscillograph records giving the time histories of each of the transducers. Inspection of these data provides estimates as to the levels, frequencies, and general quality of the data. From these records, the exact time interval for the statistical analysis was selected.

Power spectral density.- Power-spectral-density analysis yields the frequency composition of the data. Power spectral density is a measure of the mean-square value of a time history divided into relatively narrow bandwidths of frequency and has dimensions of $(\text{Quantity})^2/\text{Hz}$. The selection of the frequency bandwidths is discussed subsequently in relation to confidence statements.

Probability-density function.- The probability-density function describes the probability that the data will have values within selected bounds. To obtain a curve of probability as a function of amplitude, a summation should be taken for an infinite time interval. A more practical method with real data, used herein, is the amplitude histogram in which the data are divided into amplitude intervals and all the observations in this interval are summed and plotted as a function of the amplitude interval.

The histogram yields information such as strong sinusoidal components, nonlinearities, clipping of data, and actual peak amplitudes.

Autocorrelation function.- The autocorrelation function describes the general dependence of the amplitudes of the signals at one time relative to the amplitudes at another time. For a stationary process, the autocorrelation function is related to the power-spectral-density function by means of the Fourier transform. However, data presented in the form of autocorrelation plots point up information in a different manner from that of power-spectra plots. The autocorrelation function (1) shows sinusoidal components in the data, (2) at zero time delay is the mean-square value of the signal, and (3) at long time

delays is the mean value squared. This function was used to obtain the mean-square value for the various parameters. For vibratory motions, the mean value squared must be zero, a fact that should be verified by the computed autocorrelation function. A non-zero value indicates that further analysis of the data is necessary.

Accuracy

In the mathematics of statistics, the parameters are computed for an interval of time approaching infinity. In reality, the test time involved is finite. Therefore, the calculations can only be estimates of the true values. It is appropriate then to make some statements about the accuracy of these estimates. Listed in table II are the mathematical equations defining each of the functions of interest.

Time history.- The limitations on the time-history playback do not involve averaging and are restricted only by the amplitude and frequency-response characteristics of the galvanometer of the recorder. The galvanometers were selected to obtain the full capabilities of the data acquisition systems.

Power spectral density.- The power spectral density is a function of both the frequency bandwidth of analysis and the record length. A confidence statement about the data is also dependent on these parameters. It was assumed that the estimate of the power spectra would follow a χ^2 distribution curve (ref. 4) with the statistical degrees of freedom

$$k = 2BT \quad (1)$$

where

B bandwidth of analysis, Hz

T record length analyzed, sec

The χ^2 distribution curve for the 90-percent confidence band is shown in figure 8. Once the statistical degrees of freedom have been determined for the analysis conducted, statements giving an estimate of the reliability can be made by using this curve. For example, if the true average value of power spectra $\Phi_x(f)_{av}$ is known, figure 8 may be used to determine the 90-percent confidence limits. For an estimate having 120 statistical degrees of freedom, the measured power spectra $\Phi_x(f)_{meas}$ will fall between 0.8 and 1.22 of the true average value or within ± 1 dB of $\Phi_x(f)_{av}$. Alternately, if the power spectra $\Phi_x(f)_{meas}$ has been measured with 120 statistical degrees of freedom, then it can be stated with 90-percent confidence that the true average value is between $0.82\Phi_x(f)_{meas}$ and $1.25\Phi_x(f)_{meas}$. Additional information on this concept may be found in references 2 and 4. Since there is a limited test time for obtaining data from

the Nike firing reported herein, it is necessary to select bandwidths of analysis wide enough to obtain reasonable confidence intervals and wide enough to use the assumption of self-stationarity.

Amplitude histogram (probability density).- The amplitude histogram does not involve averaging; therefore, when using a digital approach in the data reduction, the parameter of most significance is the sampling rate. This rate is selected based on the highest frequency to be analyzed and will be specified. Although a "goodness-of-fit" test could be applied to the histogram to compare it with a known distribution, the confidence limits for such a short time period would be of such wide bounds that it was not considered a meaningful evaluation for the test reported herein.

Autocorrelation function.- The estimates of this function were assumed to follow the same distribution as power-spectral-density estimates. The method for determining the number of statistical degrees of freedom was slightly different from that used for determining power spectra and is related to the digital method of data analysis. The statistical degrees of freedom k are expressed as

$$k = 2 \frac{n}{m} \quad (2)$$

where

n sample size

m maximum number of time-lag values

The sample size is related to the record length by the following equation:

$$n = \frac{T}{\epsilon} \quad (3)$$

where

T record length analyzed, sec

ϵ sampling interval of data, sec

This value for k is identical with that evaluated for power spectra if a value of m is selected such that

$$m = \frac{1}{B\epsilon} \quad (4)$$

where

B bandwidth of analysis, Hz

The confidence intervals for the autocorrelation function are then determined in the same manner as for power spectra. The mean-square value is a particular value of the autocorrelation function and, therefore, the accuracy is also determined in the same manner.

RESULTS AND DISCUSSION

The results from the firing in the test stand are presented in figures 9 to 18. Listed in table III are the data analysis estimate parameters used in this study. Oscillograph records of measurements from the force links, displacement potentiometer, the forward and aft end Nike dc pressure transducers, the vibrometers, the forward and aft end Nike ac pressure transducers, strain gages, and microphones are presented in figure 9. Results from analysis of data from vibrometers 5 and 6 covering burn time 0.1 to 0.9 sec are shown as the acceleration power spectral density in figure 10, the amplitude histogram in figure 11, and the autocorrelation function in figure 12. Results from analysis of data from vibrometers 2, 5, and 6 covering burn time 1.2 to 2.8 sec are shown as the acceleration power spectral density in figure 13, the amplitude histogram in figure 14, and the autocorrelation function in figure 15. Analysis of data from the external microphones was conducted for approximately the entire burn time (i.e., 0.1 to 3.3 sec), and the results are shown as the acoustic power spectral density in figure 16, the amplitude histogram in figure 17, and the autocorrelation function in figure 18.

Qualitative Evaluation of Data

The oscillograph records (fig. 9) indicate that the measured data from the three force links are well within their operating range. Due to the instrumentation polarity, the recording of the measurement of force link 3 is out of phase with force links 1 and 2. (See fig. 9.) The electrical noise level of the force links, particularly link 1, is extremely high relative to oscillatory signal levels during the firing.

The displacement signal is within the anticipated range of the transducers and is consistent with the phase of the measurement of force link 3. (See fig. 9.)

The signals from vibrometers 1, 3, and 4 severely overdrove both the conditioning and recording equipment well beyond the anticipated levels, and therefore could not be analyzed. (See fig. 9.) The data from vibrometers 2, 5, and 6 appeared to be within the capabilities of the equipment and were analyzed.

The diaphragm of pressure transducer 1 failed approximately 0.24 sec after ignition; thereby all vibratory and steady-state pressure data from this transducer were lost after this time. The dc pressure measurement from transducer 3 was not recorded on the tape. The dc pressure measurement from transducer 2 is satisfactory with the exception of approximate burn time 1.92 to 2.61 sec. Although it is not known what actually caused

the problem with transducer 2 in this time period, it may be attributed either to the over-load in the power supply due to the failure of transducer 1 or to a malfunction in the pressure-transducer power supply. The ac pressures as measured from transducers 2 and 3 show a similar problem during the same time period. The oscillograph records for the ac pressure measurements do not indicate any pressure oscillations. However, the sensitivity of these transducers may not have been high enough to detect the pressure fluctuations inside the Nike case.

The strains were well within the capability of the system to record the data and are shown in figure 9. Strain gage 3 failed at approximately 2.58 sec and provided no data after that time.

The microphone data are shown in figure 9. The recording equipment was not over-driven; however, the records indicate that microphone 2 clearly has an amplitude limit.

Quantitative Evaluation of Data

Differences in event times presented in this section were obtained from high-resolution oscillograph records and are not observable in the small-scale plots in figure 9.

Force link and displacement measurements. - The static preload measured by the force links was as follows:

| | |
|--------------|---------|
| Force link 1 | 64.5 kN |
| Force link 2 | 64.5 kN |
| Force link 3 | 64.6 kN |

for a total indicated load of 193.6 kN. An initial load of 2.22 kN per link was placed on the vehicle before zeroing the force links, bringing the total preload to 200.3 kN. The maximum load as measured by the force links occurred 0.025 sec after ignition and reached an instantaneous value of 239 kN. This peak value is associated with an initial high-frequency oscillation of approximately 130 Hz. The thrust buildup near the end of the burning (approximately 2.5 sec burn time) is about 204 kN. This value includes the effects of the initial preload and the 227 kg loss in weight due to propellant burning.

The measurements of the force links indicate that the thrust of the rocket only slightly exceeded the preload and if the system had not had the retractable spacers, the rocket would have been restrained by the honeycomb stops for almost the entire firing. Although allowances were made for variations from the nominal thrust of the Nike, it was not anticipated that it would be this great. The displacement trace shows the vehicle lifting off the stops at 0.019 sec and that its initial peak value is 1.08 cm; however, the second cycle of oscillation is 1.9 cm which was the maximum displacement of the vehicle.

The frequency shown by the force links, when averaged over 0.5 sec, is 7 Hz which is in agreement with the anticipated suspension-system frequency. Evaluation of the amplitude decay at the 7-Hz frequency indicates that the damping of this mode is in the range of 3 to 4 percent of an equivalent critically damped viscous system.

Pressure measurements.- The maximum pressure of 7.65 MN/m² at the forward end of the Nike case is reached at 0.088 sec, which indicates a slower thrust buildup than anticipated. The low-frequency suspension oscillation started before the maximum pressure was reached. This may contribute to the second cycle of oscillation being greater than the initial one. Pressure transducer 1 indicated a pressure buildup at the aft end of the Nike 0.008 sec after that at the forward end. The average velocity of the pressure pulse between these two transducers is approximately 366 m/sec. The maximum pressure at the aft transducer was 7.30 MN/m².

Whereas the oscillograph records did not show any pressure oscillations, a power-spectra analysis of the ac pressure measurements did indicate signals at frequencies other than normal electrical power noise frequencies. If a normal distribution is assumed for these pressures, their estimates from the power-spectra analysis indicated that the 4-sigma peaks do not exceed 69 kN/m².

Vibration measurements.- The responses of vibrometers 2, 5, and 6 (fig. 9), which yielded usable data, show two time periods with significantly different vibration responses. The measured vibratory response, in g units, from 0.1 to 1.2 sec shows considerably higher amplitudes than those measured during the time period 1.2 sec to burnout. The amplitude histograms for vibrometer 2 indicated severe clipping of the signal, and therefore no additional analysis was conducted on these data during this time period. A power-spectra analysis was made, by use of a filter bandwidth of 40 Hz, of the longitudinal vibrations obtained from vibrometers 5 and 6 during the time period 0.1 to 0.9 sec. The results show a strong response in a frequency range from 10 000 to 10 400 Hz. (See fig. 10.) Vibrometer 5, which is at the attachment of the Nike to the payload, had a peak spectrum of 0.006 g²/Hz both in frequency band from 10 000 to 10 400 Hz and at 1600 Hz. The overall root-mean-square value for vibrometer 5 during this time was 5g_{rms}, as determined from the autocorrelation function (fig. 12), with maximum random peaks of +14.6g and -13.7g (fig. 11). The oscillations of the autocorrelation function also indicate a strong narrow-band random signal at approximately 10 000 Hz. Vibrometer 6, which is on the forward end of the payload, had a peak power spectrum of 0.038 g²/Hz. The spectrum at all other frequencies between 0 and 20 000 Hz are at least 8 dB down from the peak. The overall root-mean-square value for vibrometer 6 during this time was 8.2g_{rms}, with maximum random peaks of +38g and -29g. (See fig. 11.) The autocorrelation function (fig. 12) also indicates some 10 000-Hz random components. The amplitude histograms for vibrometers 5 and 6 (fig. 11) approximate a normal distribution. The peak values are about 3 to 4.5 times the root-mean-square value with a zero mean.

Results from analysis of the data in the time period 1.2 to 2.8 sec for vibrometer 5 show a peak power spectrum of $0.0018 \text{ g}^2/\text{Hz}$ at an approximate frequency of 1900 Hz. (See fig. 13.) The spectra are similar in magnitude and shape for the time periods analyzed except near 10 000 Hz. (Compare figs. 10 and 13.) The same can be said for vibrometer 6, with the peak spectrum being about $0.0036 \text{ g}^2/\text{Hz}$ at approximately 600 Hz. Peaks in the power spectrum at frequencies 600 Hz, 1000 Hz, 1300 Hz, and 1500 Hz can be seen in the data for both time periods. Due to the lack of a significant response near the 10 000-Hz frequency, the root-mean-square vibration levels for both vibrometers 5 and 6 are less for the later time period as are the peak accelerations. The vibration levels are $2.5 \text{ g}_{\text{rms}}$ and $4.0 \text{ g}_{\text{rms}}$ for vibrometers 5 and 6, respectively, with peak values again being in the range of 3 to 4 times the root-mean-square value. The amplitude histogram shows the distribution to be similar to a normal distribution. (See fig. 14.)

Filtering the data obtained during the first time period (0.1 to 0.9 sec) so that the response is flat to 5000 Hz and down approximately 22 dB at 10 000 Hz yields root-mean-square accelerations of $2.4 \text{ g}_{\text{rms}}$ and $3.9 \text{ g}_{\text{rms}}$ for vibrometers 5 and 6, respectively. A comparison of these values with those in the second time period (1.2 to 2.8 sec) where the levels were $2.5 \text{ g}_{\text{rms}}$ and $4.0 \text{ g}_{\text{rms}}$, respectively, shows them to be within the allowable range of ± 0.72 dB for root-mean-square values at the 90-percent confidence level for an estimate with 646 statistical degrees of freedom. (See fig. 8.) It should be remembered the mean-square value is determined from the autocorrelation function and, in using figure 8, a factor of 2 is necessary to determine confidence levels for the root-mean-square values. This agreement in the root-mean-square value is sufficient to demonstrate that the signals are weakly self-stationary (ref. 3) and, along with the agreement in the shape of the power-spectra curves, give reasonable confidence that the concept of self-stationarity for the parameters is a reasonable assumption for the bandwidths of analysis and confidence limits used in this paper.

Vibrometer 2, which is oriented in a lateral direction at the nozzle end of the vehicle, shows a decaying low-frequency oscillation of approximately 0.9 Hz on which the high-frequency oscillation is carried. The power spectrum of this signal indicates a relatively flat spectrum of $0.0008 \text{ g}^2/\text{Hz}$ up to 10 000 Hz, with a peak in the spectrum below 100 Hz. (See fig. 13.) The amplitude histogram shows a distribution which is similar in shape to a random signal with a normal distribution and a clipped sinusoidal component. (See fig. 14.) The root-mean-square acceleration determined from the autocorrelation function is 4 g_{rms} ; however, it should be noted that this function did not return to zero in the analysis time period, an indication that the mean acceleration squared is not zero. (See fig. 15.) This is due to the decaying low-frequency oscillation having a long period of oscillation compared to the analysis time and thus yielding a nonzero mean-acceleration-square value. The peak accelerations were $+7.5 \text{ g}$ and -10 g , which are about 2 to $2\frac{1}{2}$ times the root-mean-square acceleration.

Strain-gage measurements.— The outputs of the strain gages indicated a maximum strain of $430 \mu\text{m}/\text{m}$ on gage 1, which includes a response at 55 Hz during ignition through 0.4 sec. The gages then indicated relatively constant strain of $210 \mu\text{m}/\text{m}$ on gage 1, $227 \mu\text{m}/\text{m}$ on gage 2, and $252 \mu\text{m}/\text{m}$ on gage 3 until 2.6 sec; at this time the strain begins to diminish and reaches zero at 3.6 sec on all gages.

Acoustic measurements.— Both the power-spectral-density plots and the autocorrelation-function plots for the microphones indicated a response primarily at 160 Hz. (See figs. 16 and 18.) The overall sound pressure level at microphone 1 was 162 dB whereas the overall level at microphone 2 was 155 dB. However, the amplitude histogram for microphone 2 shows this transducer to be severely overdriven. (See fig. 17.) It is probable that the primary frequency is associated with a room resonant frequency since the wavelength for 160 Hz is approximately equal to the distance between the vehicle and the side walls of the test cell. It also may be observed that this acoustic level did not result in a noticeably unique response in the test vehicle at 160 Hz. (See figs. 10 and 13.)

CONCLUDING REMARKS

A firing of a Nike rocket with a boilerplate payload was conducted in a special test stand as an initial step in the investigation of the vibrational environment of solid-propellant rockets.

Since much of the data obtained during this project is random in nature, a detailed discussion of the analytical procedures used to reduce these random signals is included in this paper.

The test stand, which was designed to simulate flight boundary conditions, withstood the thrust load without failure. The average fundamental resonant frequency of the vehicle in the stand was approximately 7 Hz, well below any anticipated resonant response in the vehicle. The damping of the stand at its fundamental frequency was low enough to allow the vehicle to respond freely.

This firing had two results which had not been anticipated. First, from a viewpoint of mechanical vibration, it was expected that the frequency range of interest would be up to 5000 Hz. However, data were lost when, during the first 1.2 sec of burning, a vehicle response in the frequency range of 10 000 Hz to 10 400 Hz caused several of the vibrometer measuring systems to saturate. During the same time period, the remaining vibrometers indicated peak values as high as 38g. The significance of these high accelerations at this high frequency is difficult to evaluate. Environment specifications covering mechanical vibration seldom exceed 2000 Hz. Acoustic tests may cover this higher frequency range; however, there was no indication that this response was due to an acoustic input.

The second unanticipated result was the inability of the pressure transducers in the Nike rocket to measure the oscillatory pressure components during burning. A gain factor of 2.5 over the steady-state pressures was far too low to detect pressure oscillations. Evaluation of the pressure data indicated that the peak values of pressure were below 69 kN/m² and could not be accurately detected by these transducers. Since these very low pressure oscillations caused vibration levels which were easily detected, improvement in the pressure detecting system is required in order to correlate input with response.

Analysis of data from two vibrometers indicated that the acceleration power spectra in the frequency range below 5000 Hz varied little between burn time 0.1 to 0.9 sec and burn time 1.2 to 2.8 sec. This agreement in both frequency and amplitude, along with agreement of the root-mean-square value of vibratory accelerations in these frequency ranges, provides the verification of the original assumption of self-stationarity. The power spectra indicated peak responses at approximately 600 Hz, 1000 Hz, 1300 Hz, and 1500 Hz for both the vibrometers. The maximum power spectrum for the vibrometer at the Nike-payload attachment was 0.0018 g²/Hz and occurred at approximately 1900 Hz. The maximum power spectrum for the vibrometer on the forward end of the payload was about 0.0036 g²/Hz at approximately 600 Hz.

Langley Research Center,
National Aeronautics and Space Administration,
Hampton, Va., September 30, 1971.

REFERENCES

1. Neff, W. J.; and Montes de Oca, R. A.: Launch Environment Profiles for Sounding Rockets and Spacecraft. NASA TN D-1916, 1964.
2. Bendat, Julius S.; and Piersol, Allan G.: Measurement and Analysis of Random Data. John Wiley & Sons, Inc., c.1966.
3. Houbolt, John C.; Steiner, Roy; and Pratt, Kermit G.: Dynamic Response of Airplanes to Atmospheric Turbulence Including Flight Data on Input and Response. NASA TR R-199, 1964.
4. Blackman, R. B.; and Tukey, J. W.: The Measurement of Power Spectra. Dover Publ., Inc., 1959.

TABLE I.- OPERATING RANGE AND CALIBRATIONS
FOR THE DATA MEASURING SYSTEMS

| Instrument | Linear operating range | | Calibrate signal | |
|----------------------------|---------------------------|------------------|---------------------------|------------------|
| | Amplitude | Frequency, Hz | Amplitude | Frequency, Hz |
| Force link 1 | 80 kN | 0 to 500 | 64.5 kN | dc |
| Force link 2 | 80 kN | 0 to 500 | 64.5 kN | dc |
| Force link 3 | 80 kN | 0 to 500 | 64.6 kN | dc |
| Displacement potentiometer | 15 cm | 0 to 100 | 8.62 cm | dc |
| ac pressure measurement 1 | $\pm 2.07 \text{ MN/m}^2$ | 40 to 3000 | $\pm 2.07 \text{ MN/m}^2$ | $\pm \text{dc}$ |
| ac pressure measurement 2 | $\pm 2.07 \text{ MN/m}^2$ | 40 to 3000 | $\pm 2.07 \text{ MN/m}^2$ | $\pm \text{dc}$ |
| ac pressure measurement 3 | $\pm 2.07 \text{ MN/m}^2$ | 40 to 3000 | $\pm 2.07 \text{ MN/m}^2$ | $\pm \text{dc}$ |
| dc pressure measurement 1 | 10.18 MN/m^2 | 0 to 5000 | 10.18 MN/m^2 | dc |
| dc pressure measurement 2 | 10.63 MN/m^2 | 0 to 5000 | 10.63 MN/m^2 | dc |
| Vibrometer 1 | $\pm 14g$ | 3 to 5000 | $\pm 10g$ | 1000 |
| Vibrometer 2 | $\pm 14g$ | 3 to 5000 | $\pm 10g$ | 1000 |
| Vibrometer 3 | $\pm 14g$ | 3 to 5000 | $\pm 10g$ | 1000 |
| Vibrometer 4 | $\pm 14g$ | 3 to 5000 | $\pm 10g$ | 1000 |
| Vibrometer 5 | $\pm 14g$ | 3 to 5000 | $\pm 10g$ | 1000 |
| Vibrometer 6 | $\pm 42g$ | 3 to 5000 | $\pm 30g$ | 1000 |
| Strain gage 1 | $1000 \mu\text{m/m}$ | 0 to 1000 | $600 \mu\text{m/m}$ | dc |
| Strain gage 2 | $1000 \mu\text{m/m}$ | 0 to 1000 | $600 \mu\text{m/m}$ | dc |
| Strain gage 3 | $1000 \mu\text{m/m}$ | 0 to 1000 | $600 \mu\text{m/m}$ | dc |
| Microphone 1 | 180 dB | 10 000 | 150 dB | 1000 |
| Microphone 2 | 150 dB | 10 000 | 140 dB | 1000 |

Note: The vibrometer measuring system was within 1.2 dB at 10 000 Hz.

TABLE II.- PROPERTIES OF EXPERIMENTAL DATA

Time history:

$$x = f(t)$$

Power spectral density:

$$\Phi_x(f) = \lim_{\Delta f \rightarrow 0} \lim_{T \rightarrow \infty} \frac{1}{(\Delta f)(T)} \int_0^T x^2(t, f, \Delta f) dt$$

Probability density:

$$p(x) = \lim_{\Delta x \rightarrow 0} \lim_{T \rightarrow \infty} \frac{1}{T} \left(\frac{T_x}{\Delta x} \right)$$

Autocorrelation:

$$R_x(\tau) = \lim_{T \rightarrow \infty} \frac{1}{T} \int_0^T x(t) x(t+\tau) dt$$

Mean-square value:

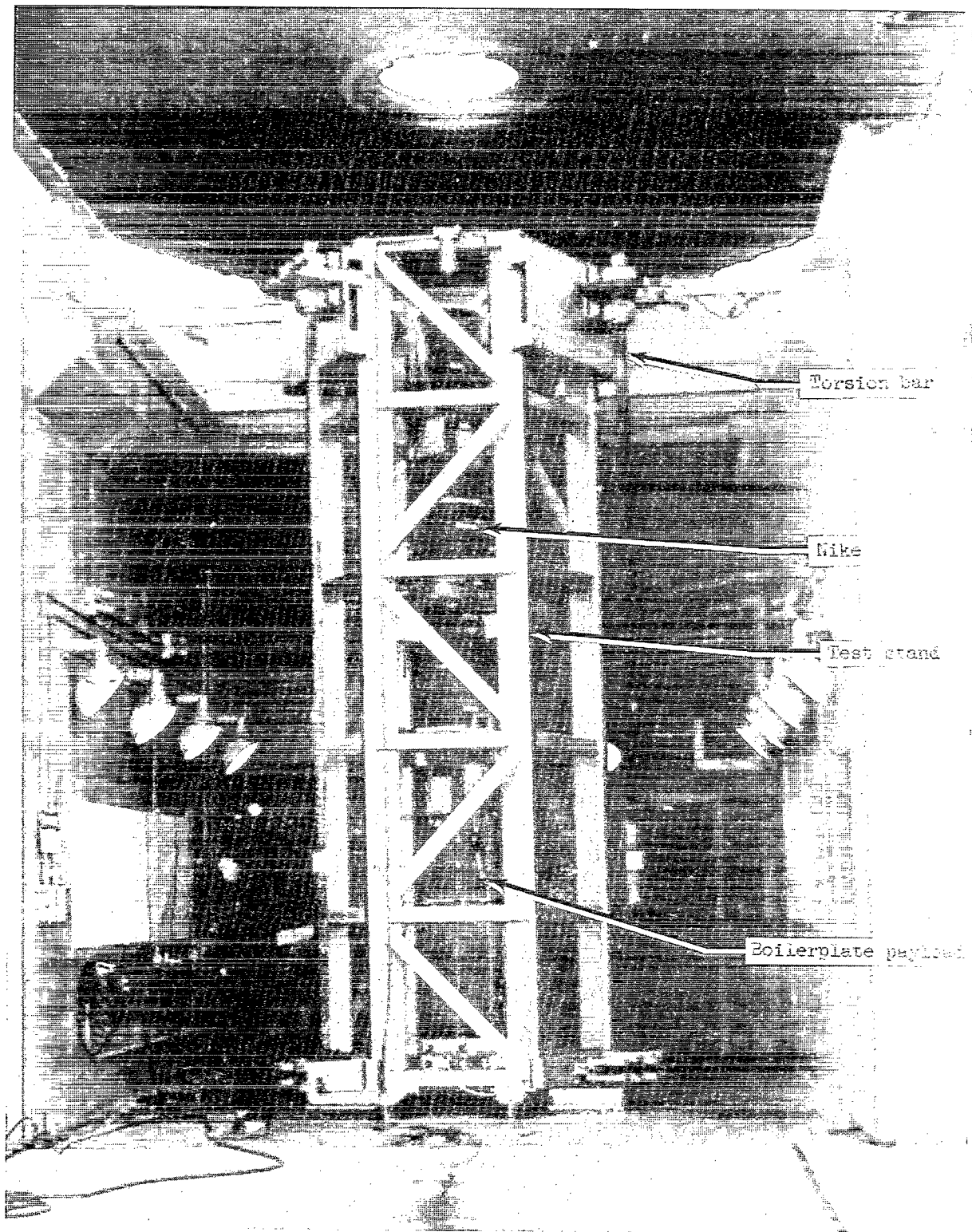
$$\sigma_x^2 = \lim_{T \rightarrow \infty} \frac{1}{T} \int_0^T x^2(t) dt$$

Mean value:

$$\mu_x = \lim_{T \rightarrow \infty} \frac{1}{T} \int_0^T x(t) dt$$

TABLE III.- DATA ANALYSIS ESTIMATE PARAMETERS

| | |
|-----------------------------------------------------|------------------------------------------------------------------------------------------------------------------------------------------------------------|
| Galvanometer response | Flat, 0 to 10 000 Hz |
| Data analyzed during burn times | $\begin{cases} 0.1 \text{ to } 0.9 \text{ sec } (\Delta t = 0.8 \text{ sec}) \\ 1.2 \text{ to } 2.8 \text{ sec } (\Delta t = 1.6 \text{ sec}) \end{cases}$ |
| Power spectra: | |
| Frequency range | 0 to 20 000 Hz |
| Bandwidth, B | 40 Hz |
| Degrees of freedom, k, for - | |
| Burn time 0.1 to 0.9 sec | 64 |
| Burn time 1.2 to 2.8 sec | 128 |
| Amplitude histogram: | |
| Burn time, sec | 0.1 to 0.9 1.2 to 2.8 |
| Sampling interval, ϵ , μ sec | 25 100 |
| Autocorrelation: | |
| Burn time, sec | 0.1 to 0.9 1.2 to 2.8 |
| Sampling interval, ϵ , μ sec | 25 100 |
| Maximum number of time-lag values, m | 99 99 |
| Sample size, n | 32 000 16 000 |
| Degrees of freedom, k | 646 323 |
| Bandwidth, B, Hz | 401 101 |



L-70-8341.1

Figure 1.- Rocket test stand and payload.

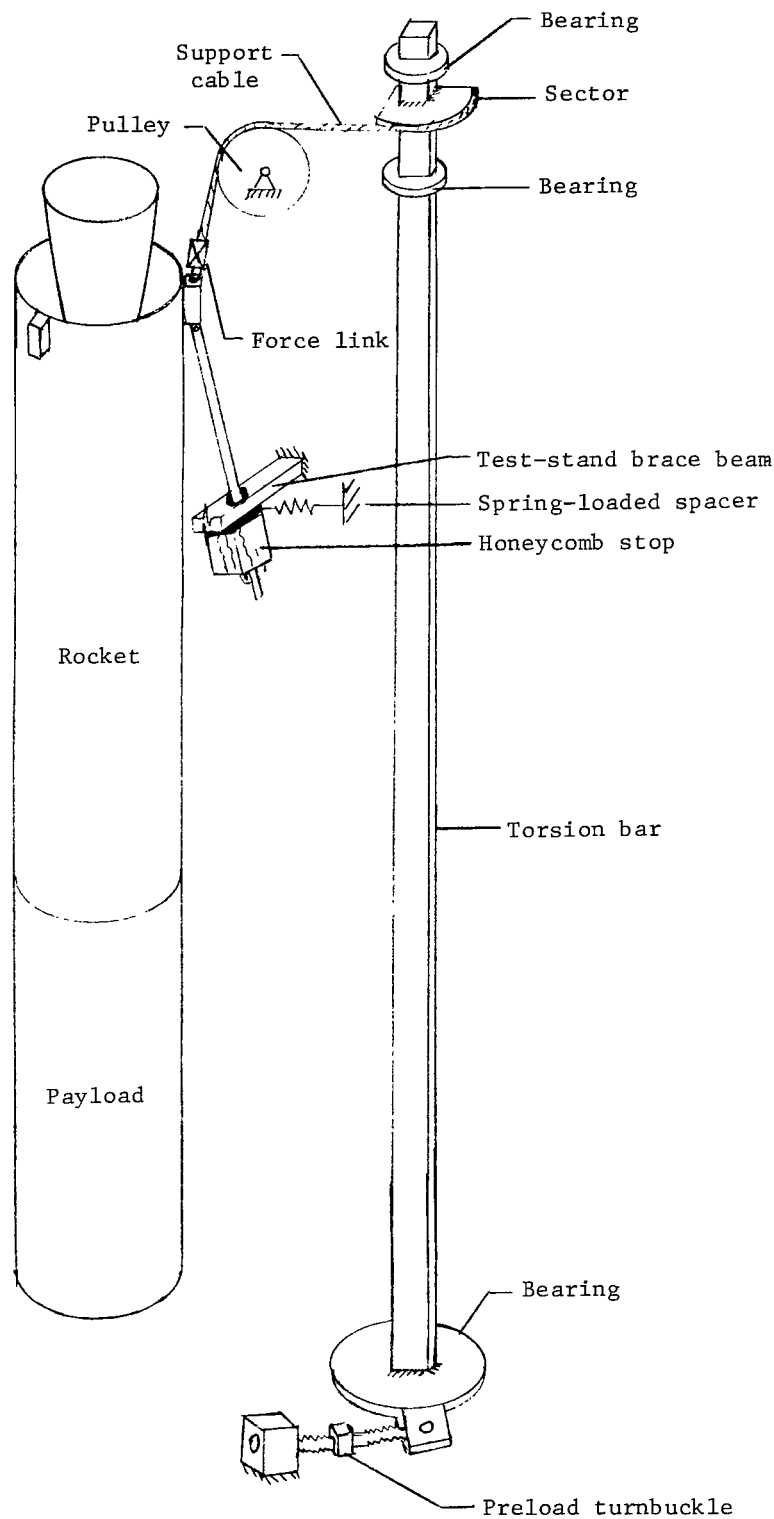
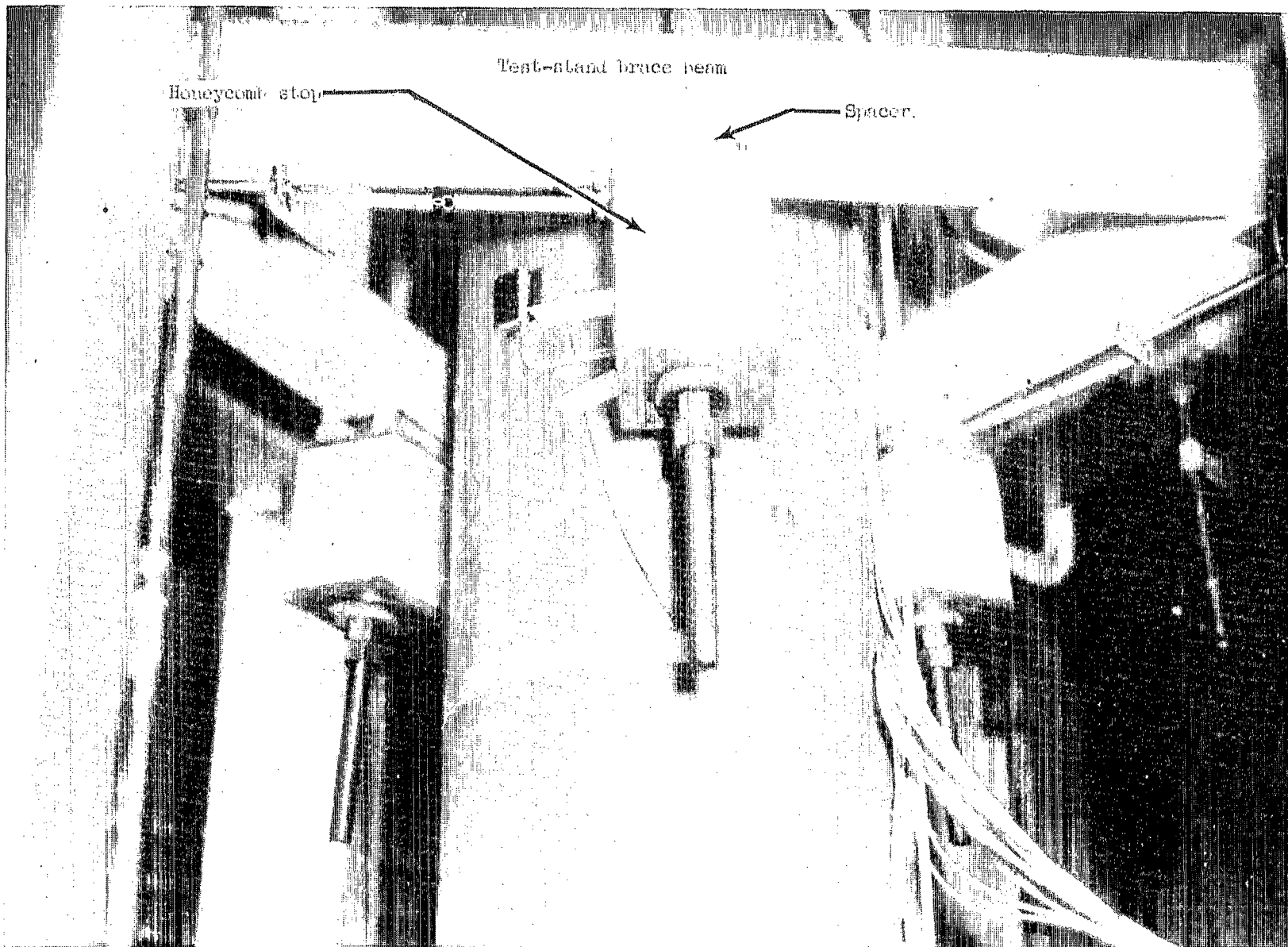
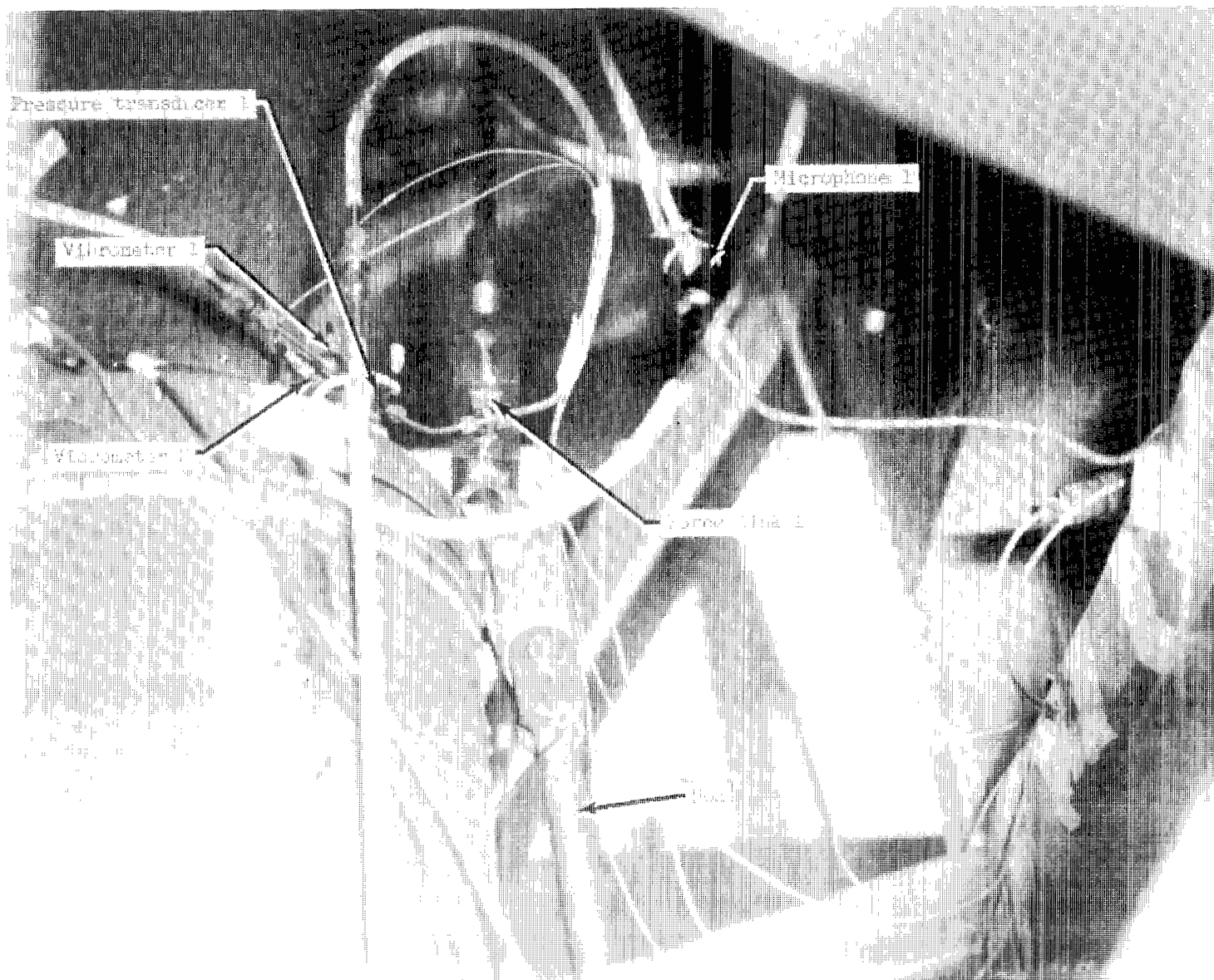


Figure 2.- Schematic view of torsion-bar support system.



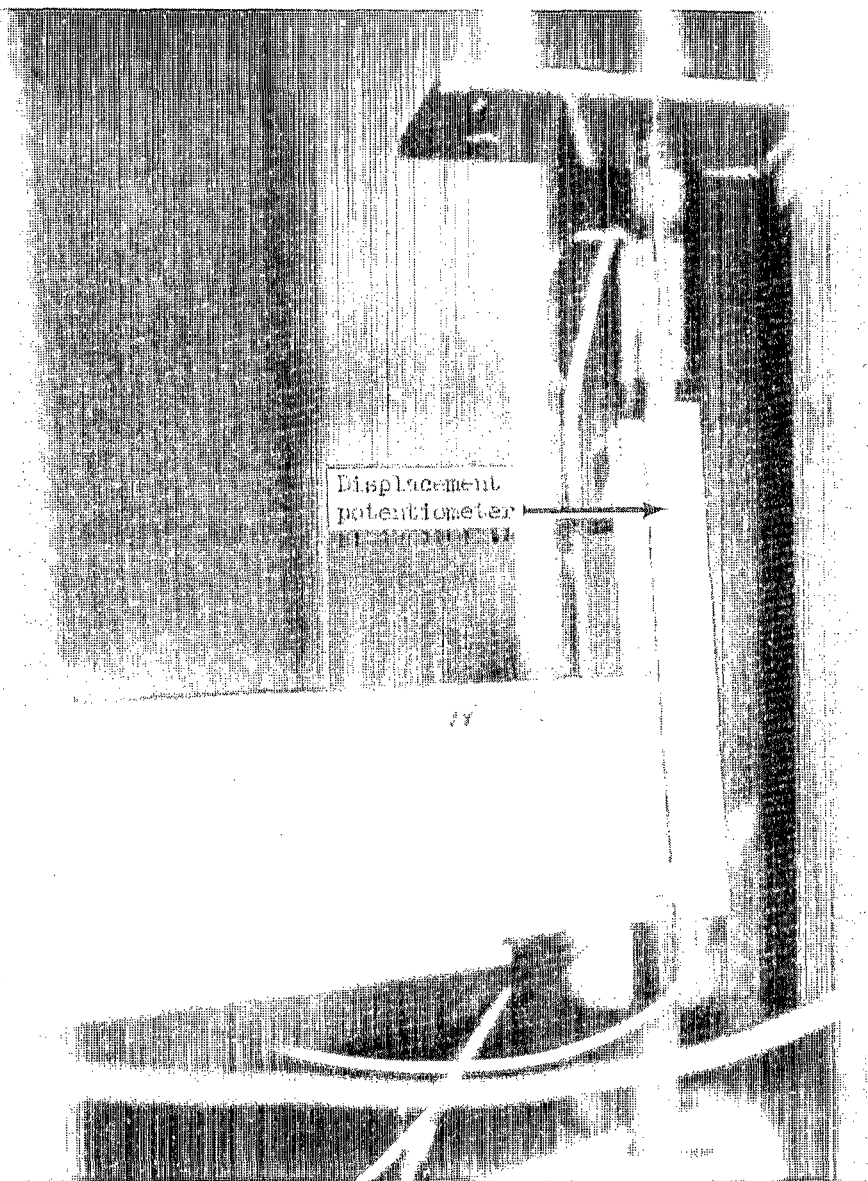
L-70-8348.1

Figure 3.- Honeycomb stop and spring-loaded spacers.



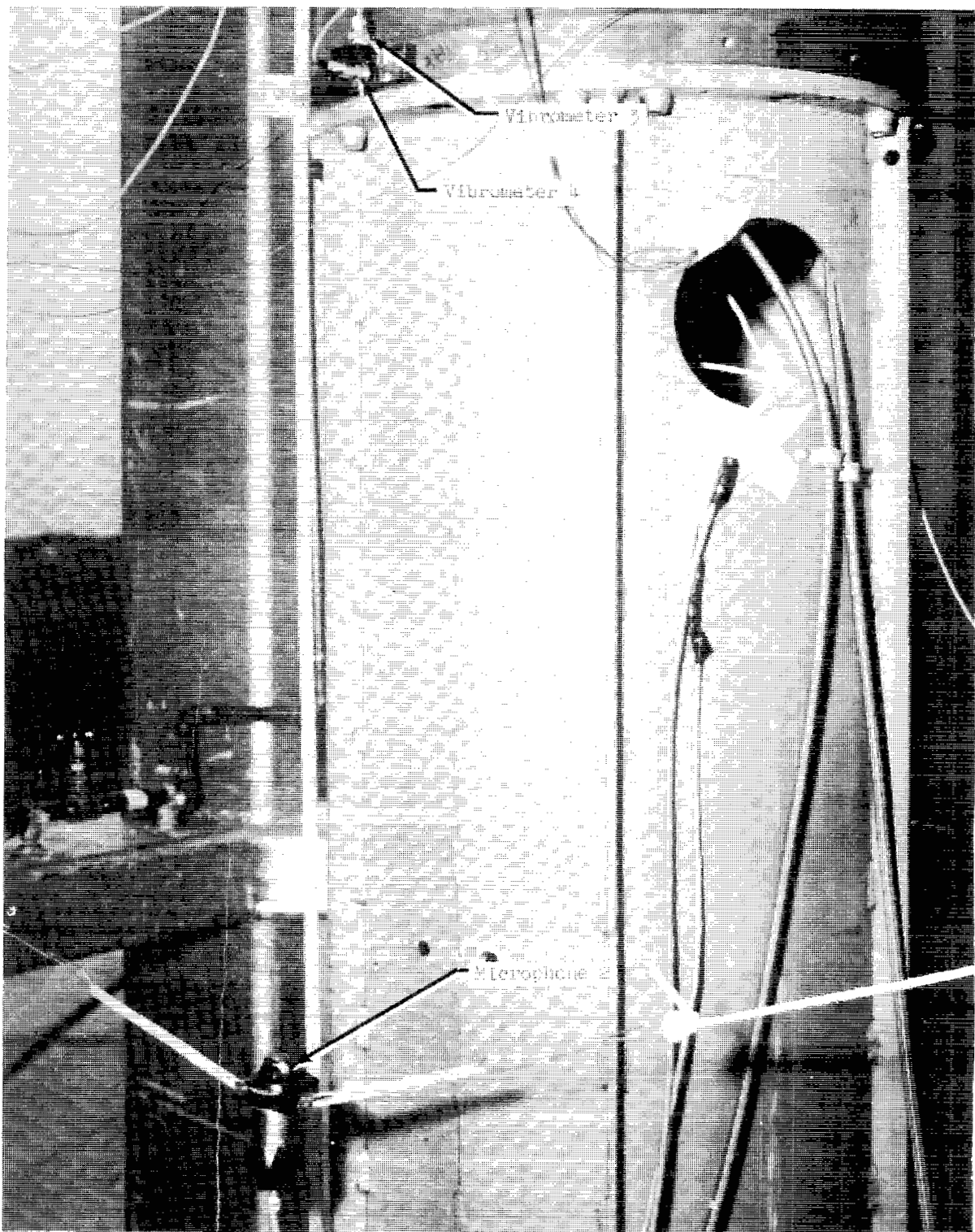
L-70-8347.1

Figure 4.- Aft end of test vehicle in test stand.



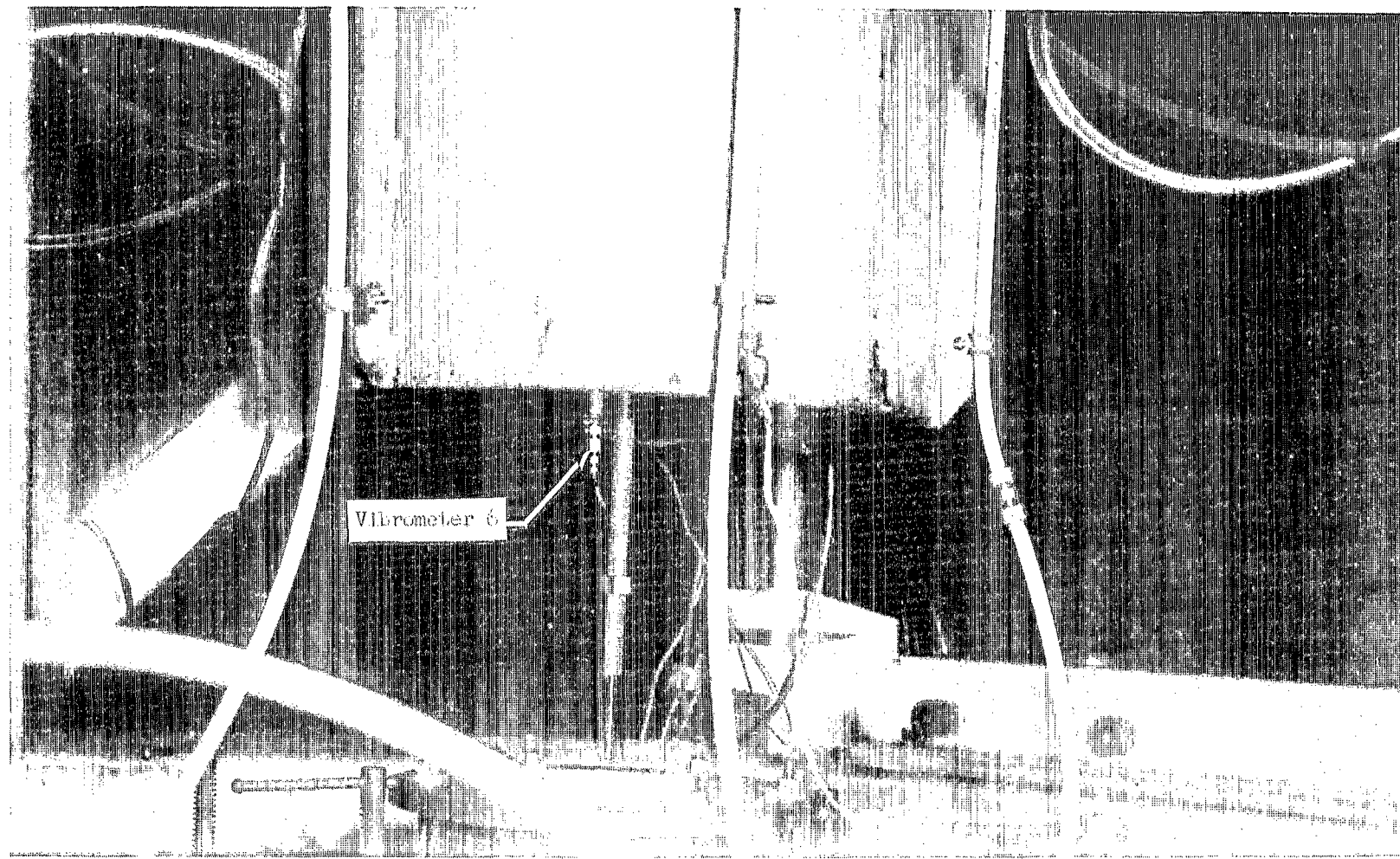
L-70-8346.1

Figure 5.- Displacement potentiometer.



L-70-8343.1

Figure 6.- Vibrometers at forward end of Nike and microphone near midpoint of payload.



L-70-8345.1

Figure 7.- Vibrometer on forward end of payload.

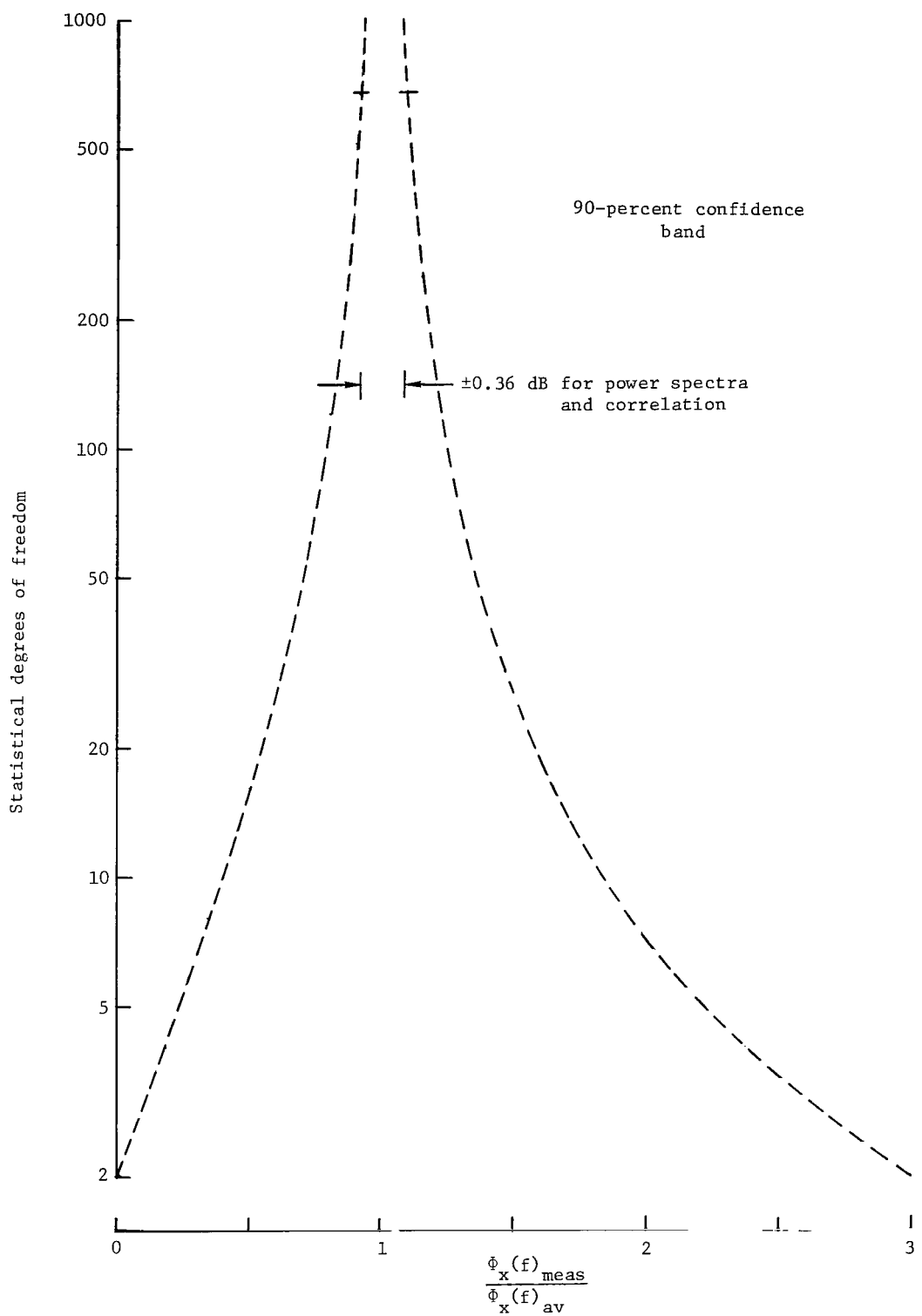


Figure 8.- χ^2 distribution curve for estimates of power spectra and correlation.

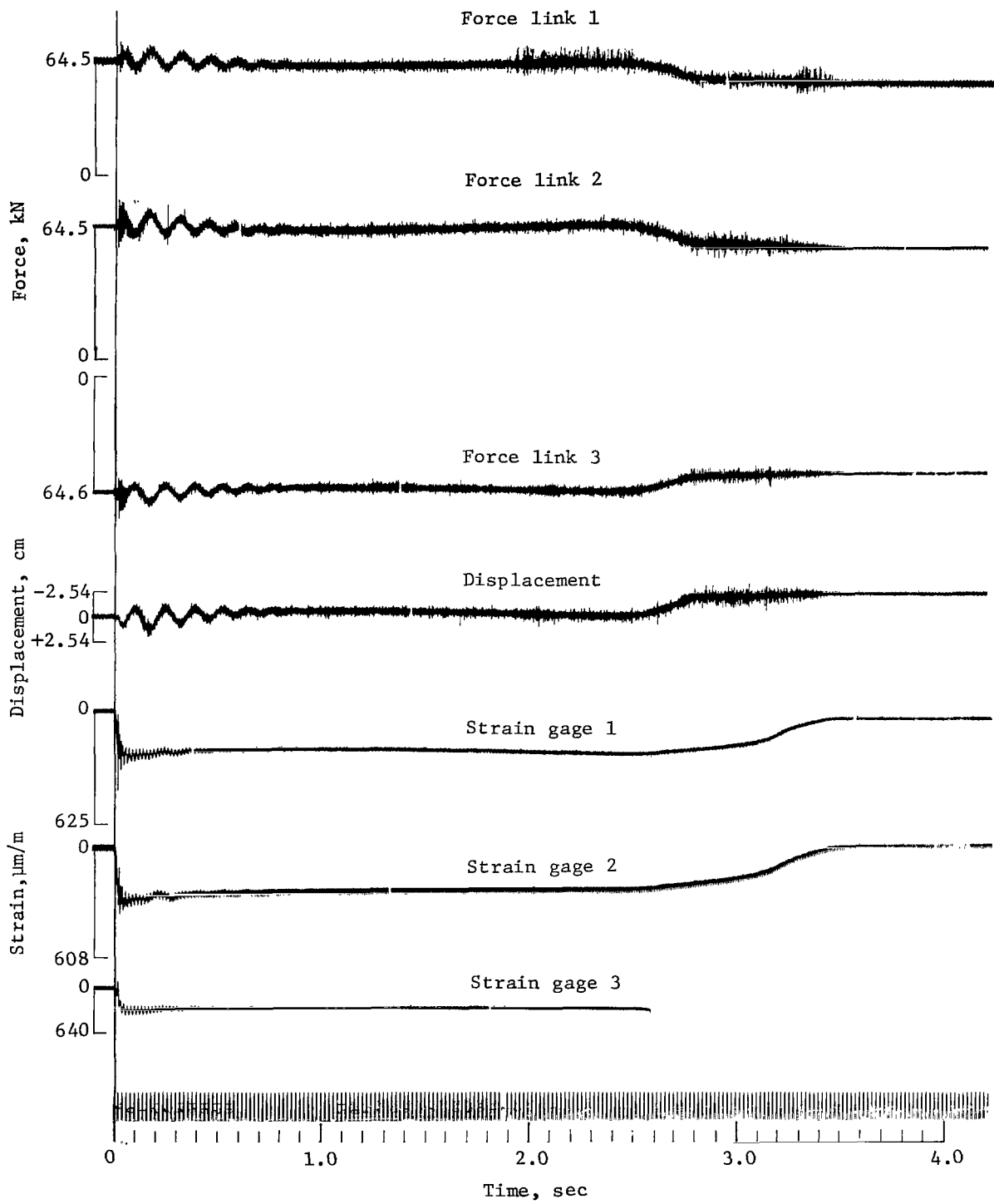


Figure 9.- Oscillograph records of data from Nike firing in test stand.

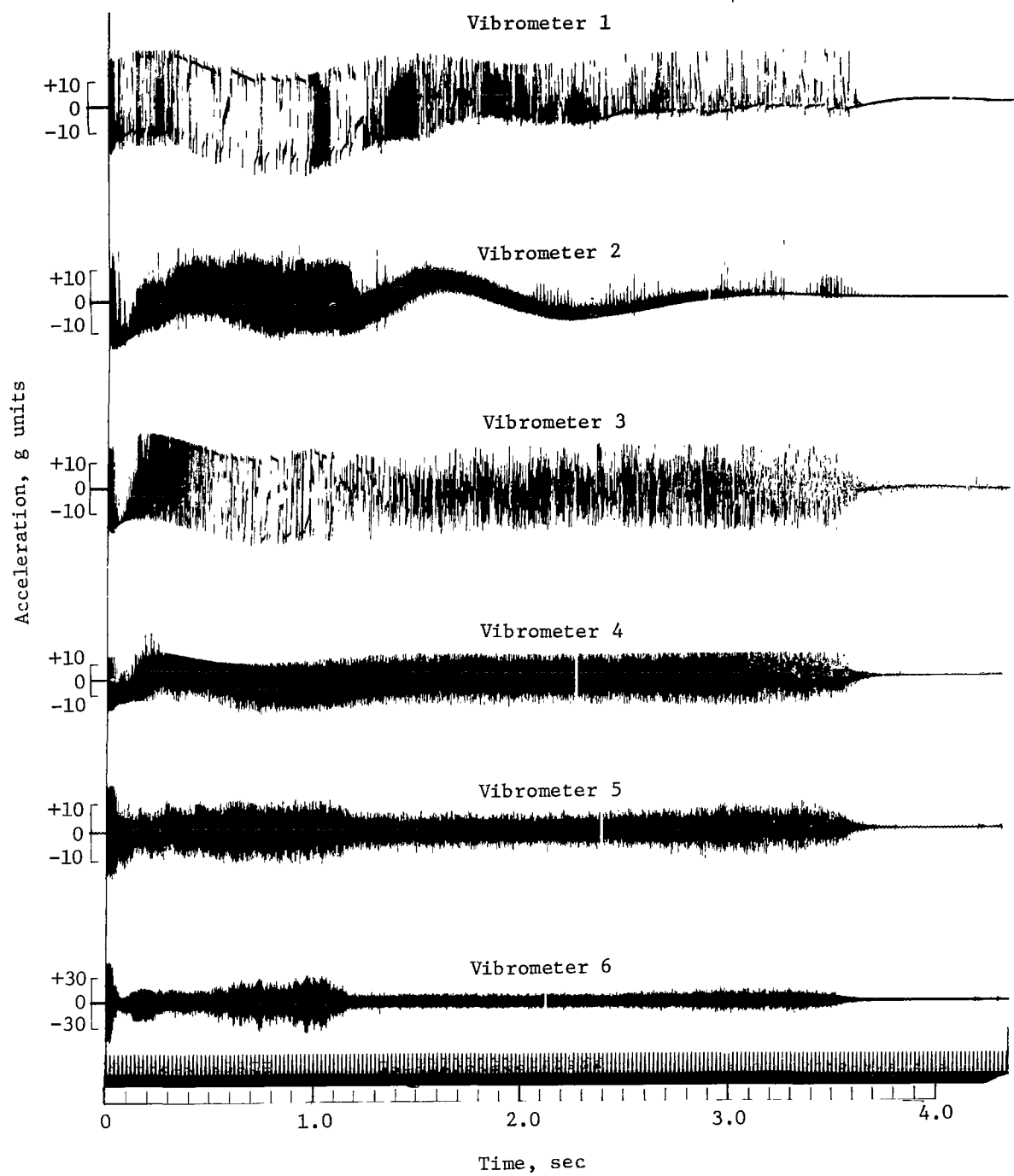


Figure 9.- Continued.

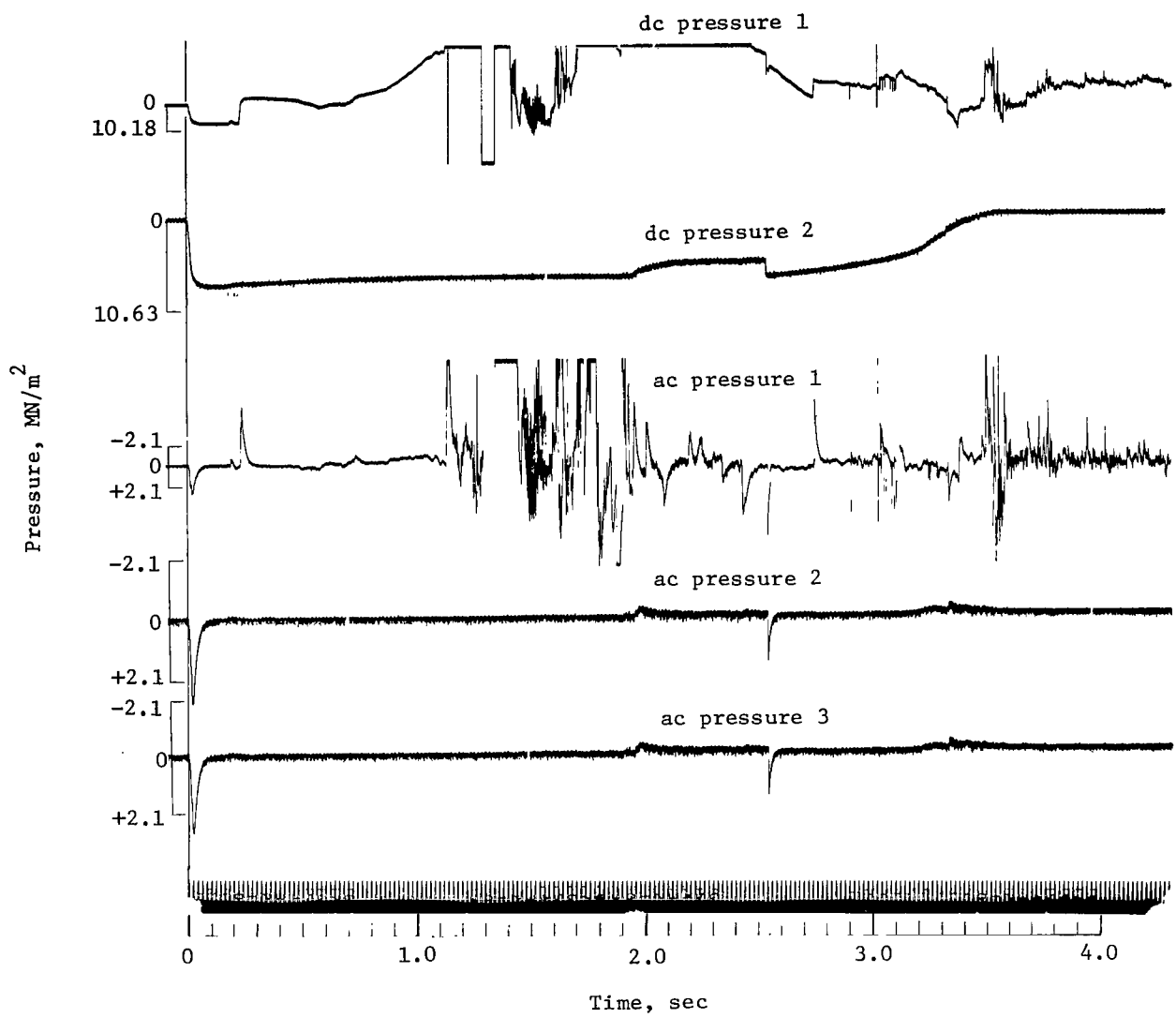


Figure 9.- Continued.

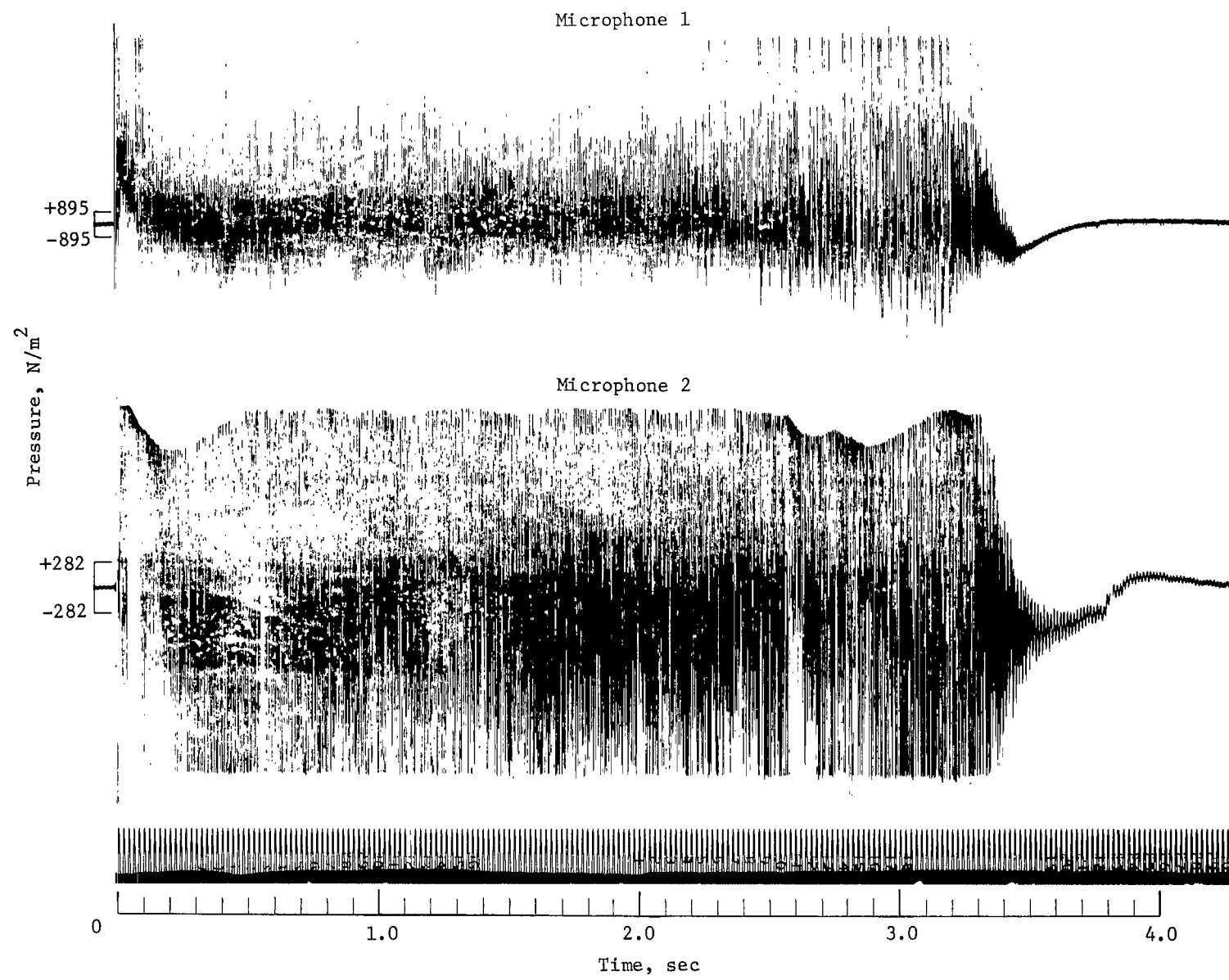


Figure 9.- Concluded.

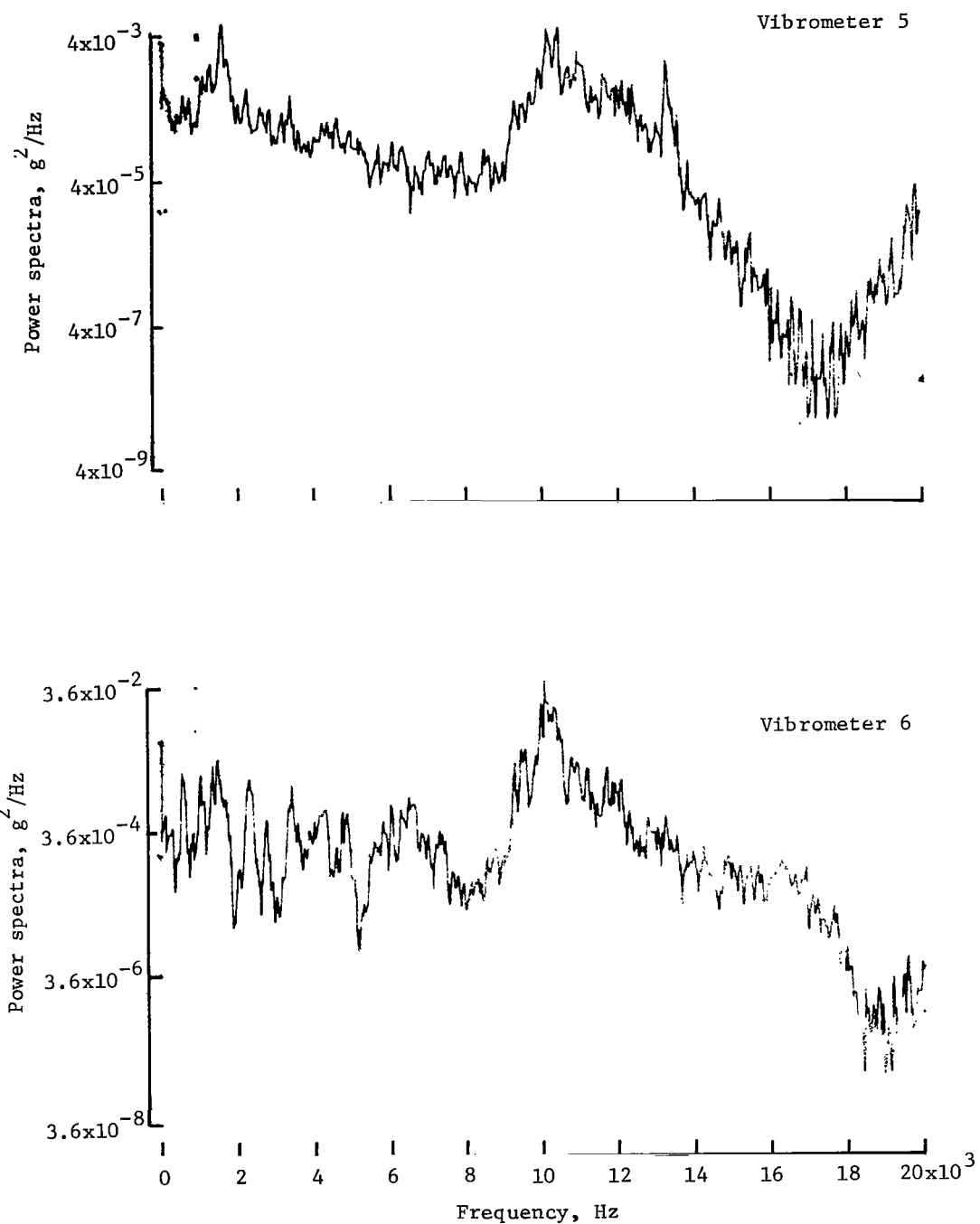


Figure 10.- Vibrometer acceleration power spectra for burn time 0.1 to 0.9 sec.

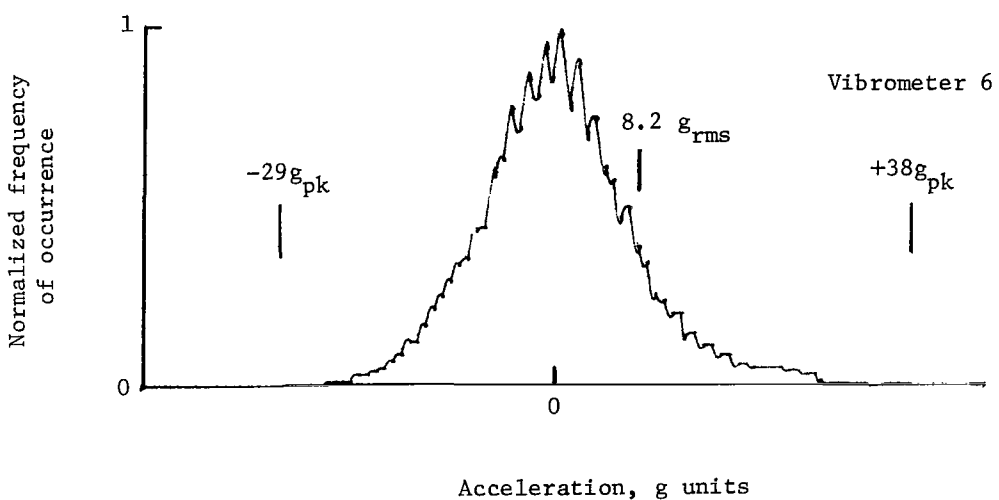
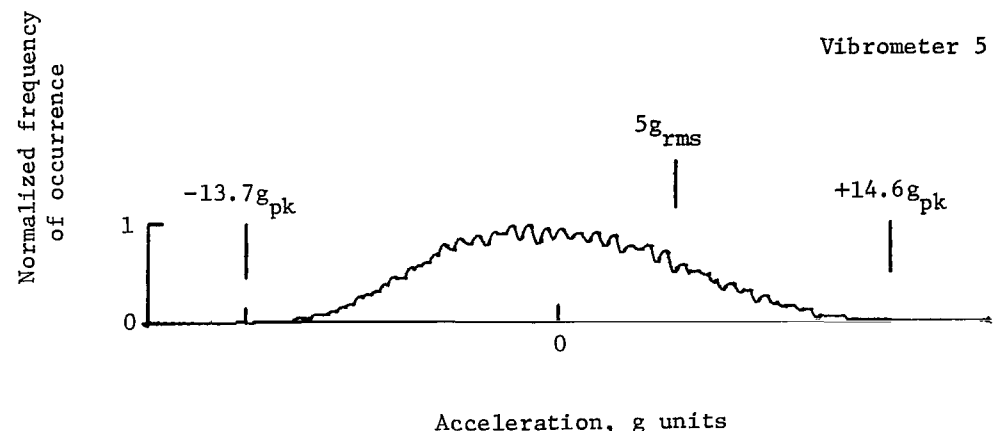


Figure 11.- Vibrometer acceleration histogram for burn time 0.1 to 0.9 sec.

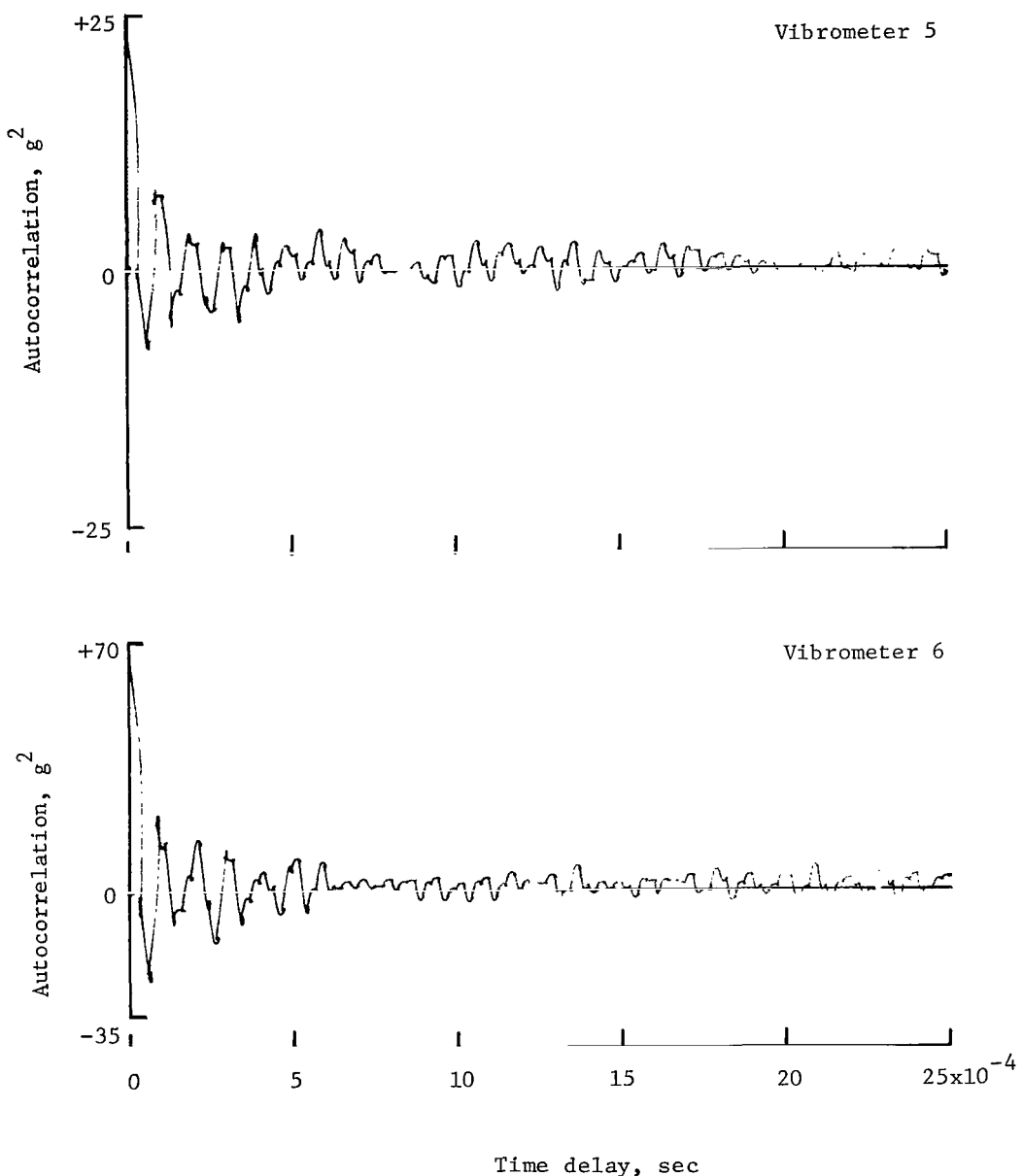


Figure 12.- Vibrometer autocorrelation function for burn time 0.1 to 0.9 sec.

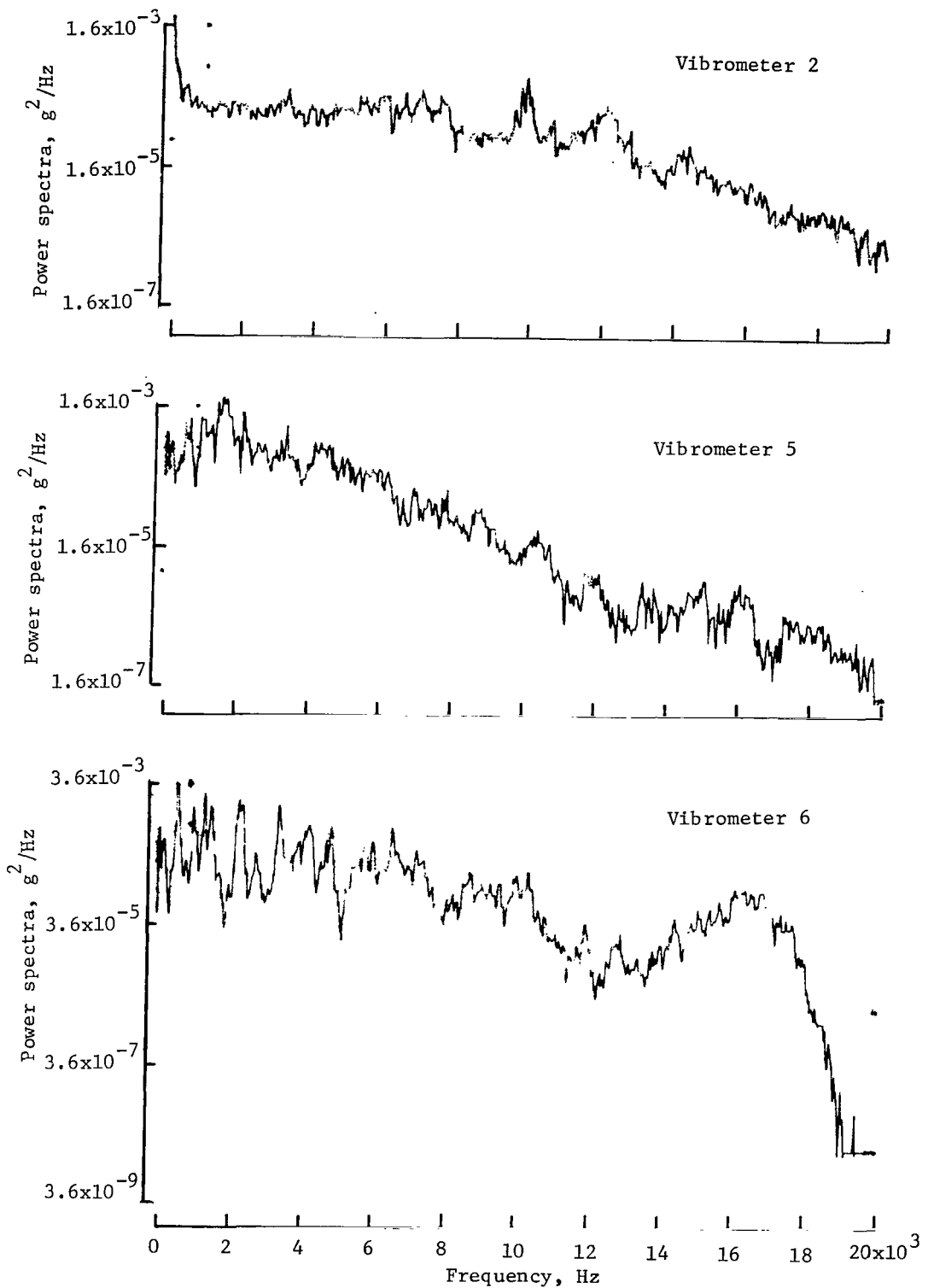


Figure 13.- Vibrometer acceleration power spectra for burn time 1.2 to 2.8 sec.

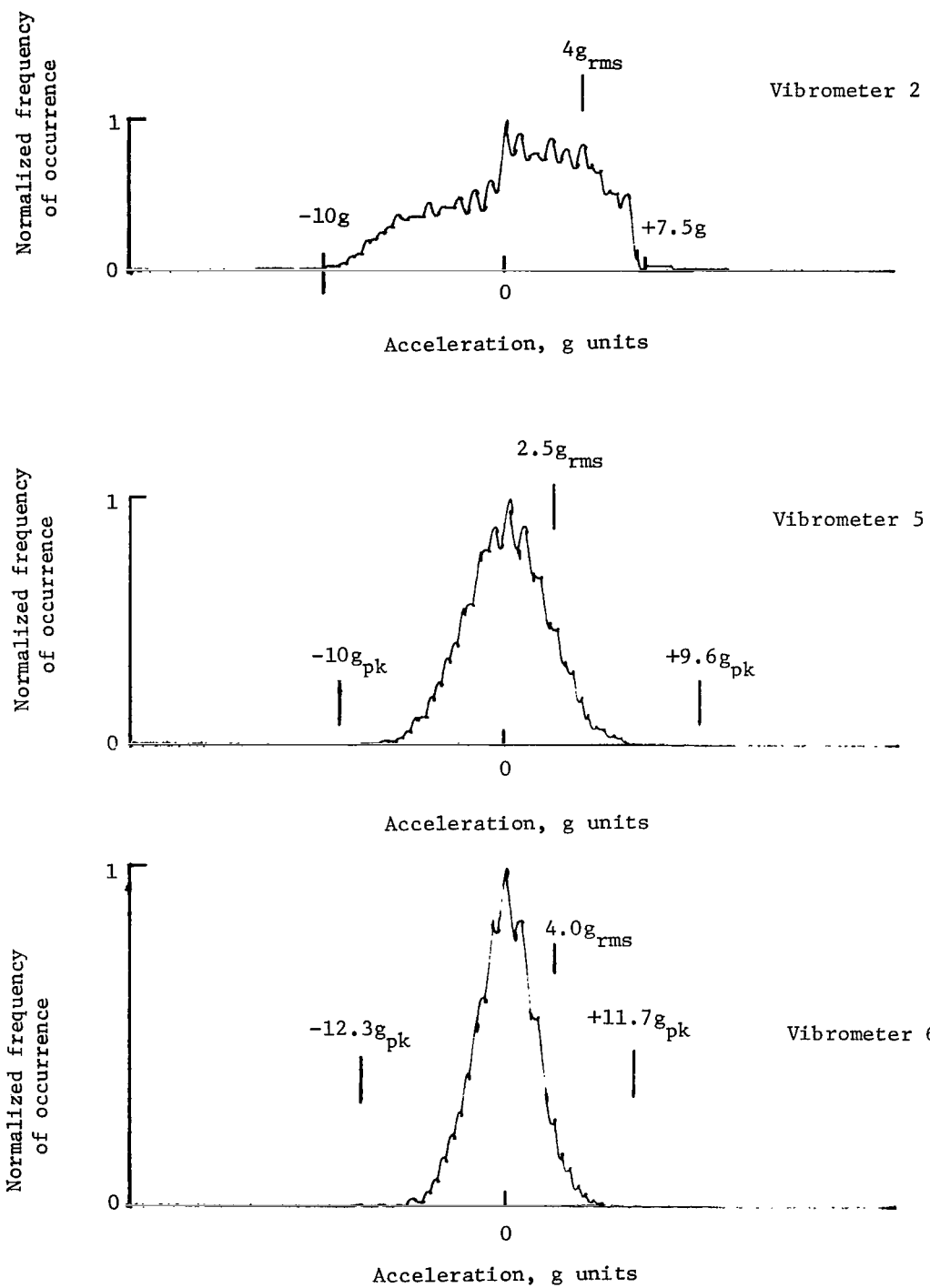


Figure 14.- Vibrometer acceleration histogram for burn time 1.2 to 2.8 sec.

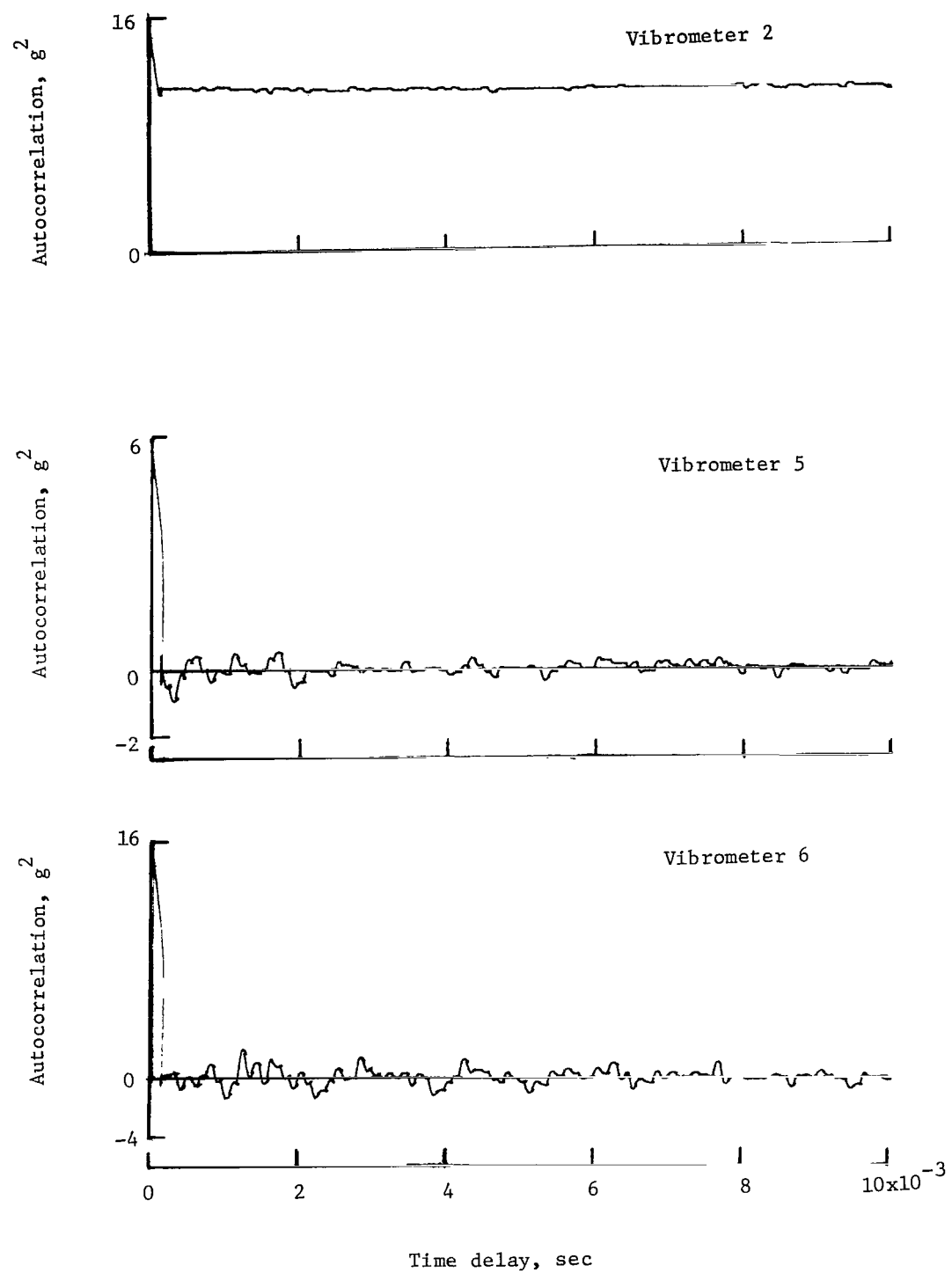


Figure 15.- Vibrometer autocorrelation function for burn time 1.2 to 2.8 sec.

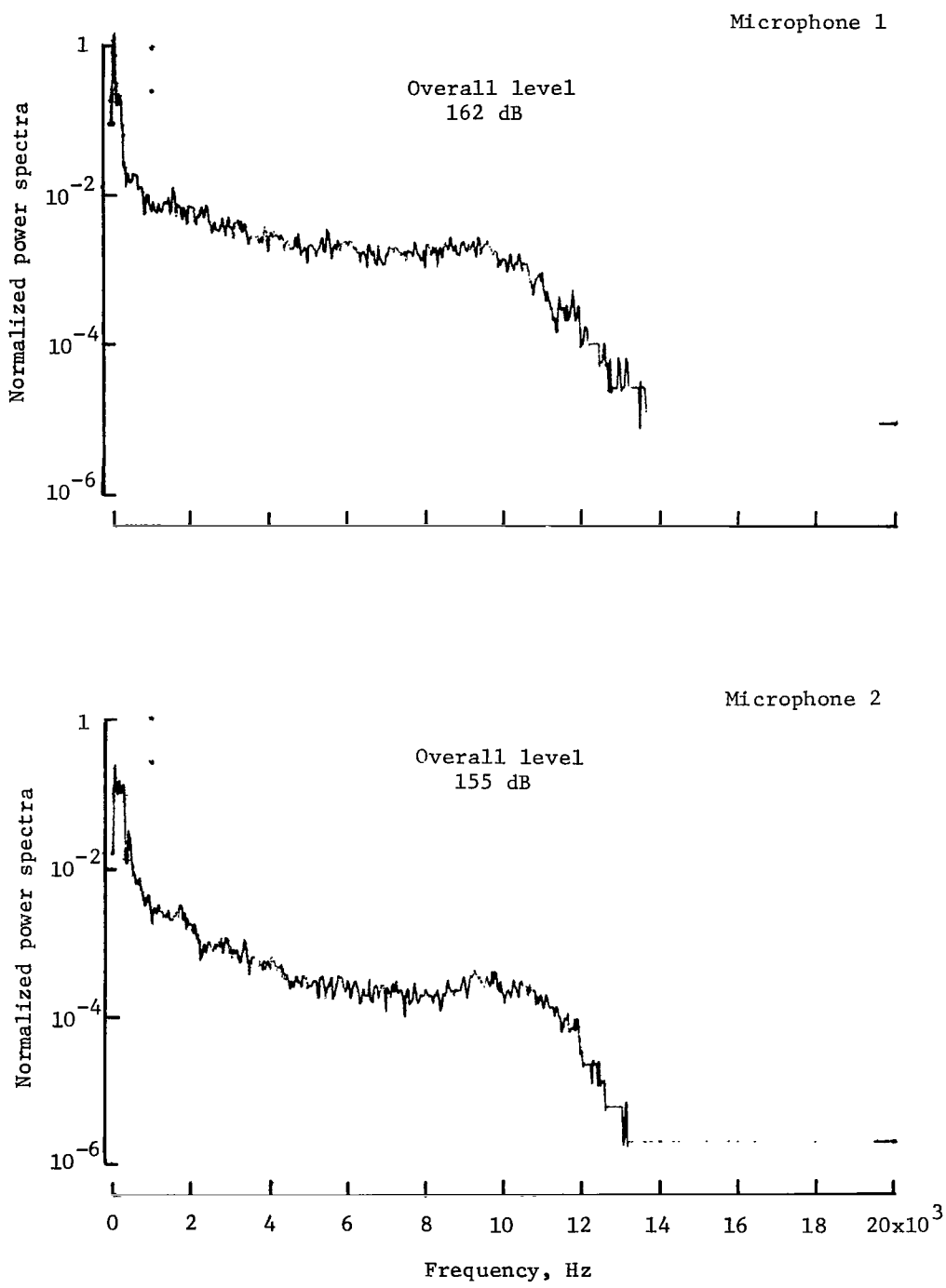


Figure 16.- Acoustic power spectra.

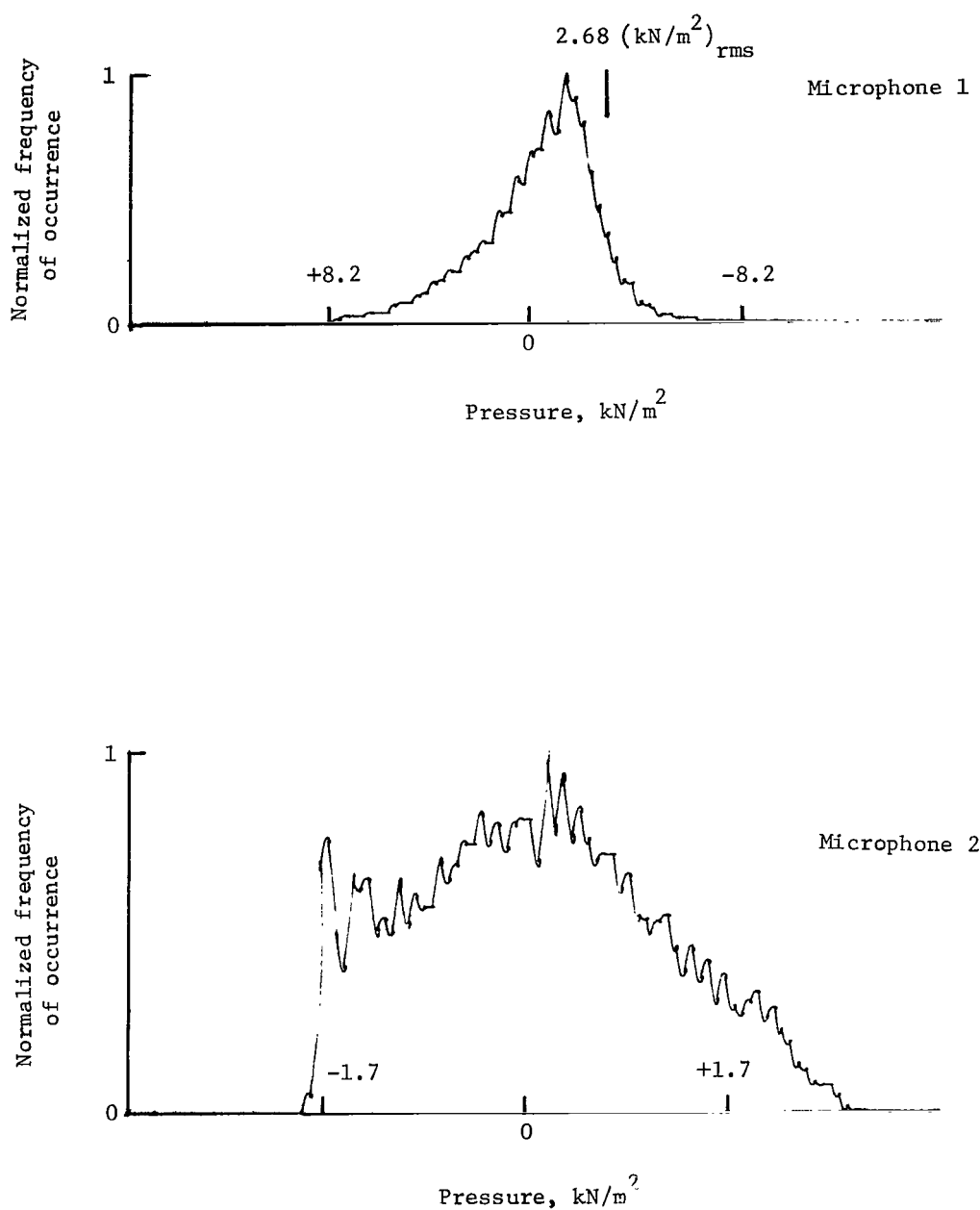


Figure 17.- Acoustic pressure histogram.

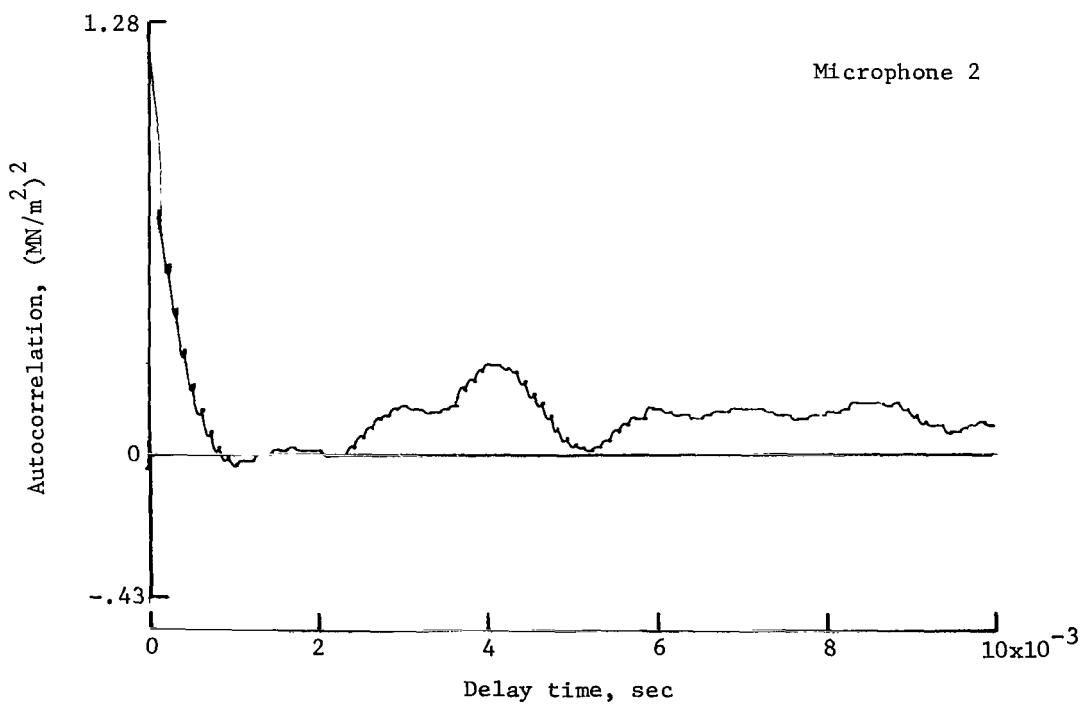
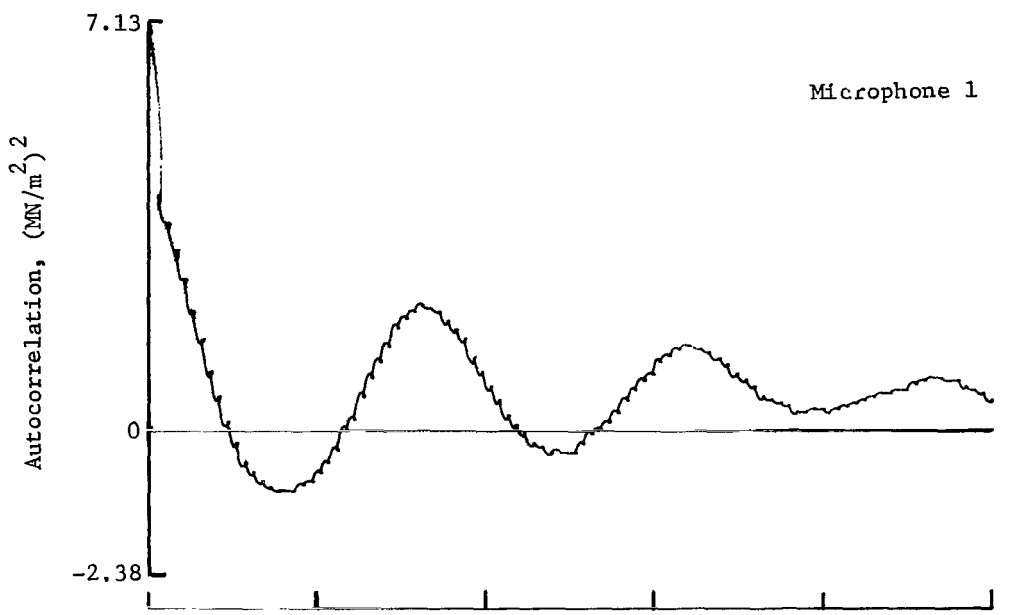


Figure 18.- Acoustic pressure autocorrelation.



015 001 C1 U 32 711015 S00903DS
DEPT OF THE AIR FORCE
AF WEAPONS LAB (AFSC)
TECH LIBRARY/WLOL/
ATTN: E LOU BOWMAN, CHIEF
KIRTLAND AFB NM 87117

POSTMASTER: If Undeliverable (Section 158
Postal Manual) Do Not Return

"The aeronautical and space activities of the United States shall be conducted so as to contribute . . . to the expansion of human knowledge of phenomena in the atmosphere and space. The Administration shall provide for the widest practicable and appropriate dissemination of information concerning its activities and the results thereof."

— NATIONAL AERONAUTICS AND SPACE ACT OF 1958

NASA SCIENTIFIC AND TECHNICAL PUBLICATIONS

TECHNICAL REPORTS: Scientific and technical information considered important, complete, and a lasting contribution to existing knowledge.

TECHNICAL NOTES: Information less broad in scope but nevertheless of importance as a contribution to existing knowledge.

TECHNICAL MEMORANDUMS:
Information receiving limited distribution because of preliminary data, security classification, or other reasons.

CONTRACTOR REPORTS: Scientific and technical information generated under a NASA contract or grant and considered an important contribution to existing knowledge.

TECHNICAL TRANSLATIONS: Information published in a foreign language considered to merit NASA distribution in English.

SPECIAL PUBLICATIONS: Information derived from or of value to NASA activities. Publications include conference proceedings, monographs, data compilations, handbooks, sourcebooks, and special bibliographies.

TECHNOLOGY UTILIZATION PUBLICATIONS: Information on technology used by NASA that may be of particular interest in commercial and other non-aerospace applications. Publications include Tech Briefs, Technology Utilization Reports and Technology Surveys.

Details on the availability of these publications may be obtained from:

SCIENTIFIC AND TECHNICAL INFORMATION OFFICE

NATIONAL AERONAUTICS AND SPACE ADMINISTRATION
Washington, D.C. 20546